CHAPTER 5
The Slippage Event

1. Introduction

It was previously observed (chapter 4) that the pile and the soil interaction suffered from a continuously coupled behaviour during the use of the simple 1D model (chapter 3). This modelling constraint perturbs the back-analysis process and the quality of the optimisation. It was concluded from these results that the slippage between the pile in the soil during a loading test was required and must be implemented in the pile/soil model. But the character of the 1D model prohibits this evolution since the model is developed in only one degree of freedom: the pile one.

Indeed, with the slippage modelling comes another need: the introduction of the soil motion, independently of the pile motion while slippage happens. This introduction brings on a second degree of freedom and complicates the scheme of resolution of the 1D model described in chapter 3. In order to introduce this second degree of freedom, assumptions must be set to describe the soil concerned. Is it only the soil reaction acting at the interface or the soil until a large distance where the effects of the pile loading are not felt?

This section intends to open different ways in order to take slippage into account in the shaft friction modelling and to study the behaviour of the soil in the direct vicinity of the pile during the slippage according to the modelling assumptions assessed. Two approaches are followed focused on the shaft friction modelling, only concerned by the slippage.

First, only the soil reaction in the direct vicinity of the pile is taken into account: the soil reaction interacting directly in the pile equilibrium. A model including the own motion of the soil is presented. This model is called the DDOF for Double Degree Of Freedom, to be compared with the 1D model of chapter 3 called in this chapter the SDOF model (for Single Degree Of Freedom). The DDOF model has two motion systems, but no horizontal development. The soil behaviour concerns only the highly perturbed zone.

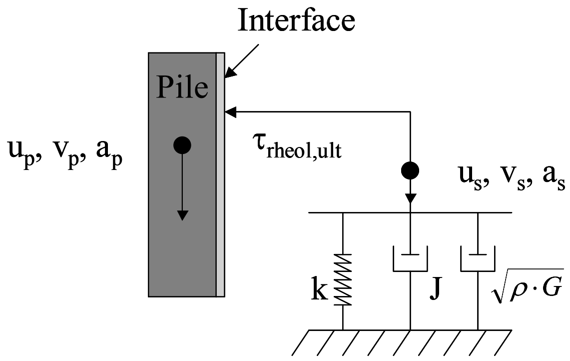

Figure V-1 : Schematic description of the ML model

The soil reaction is modelled similarly to the SDOF model by using mechanical devices: a non-linear spring and two dashpots for the viscous and the radiation term representing the soil impedance (Figure V-1). The slippage event is marked by the coupling and re-bonding of both pile and soil surfaces.

Second, the soil is described horizontally by means of a cylindrical development of the SDOF model (Figure V-2). The pile is located in the centre of concentric cylinders representing the soil. The cylinders are a set of rings with same thickness and increasing height. The last ring closes the model by an absorbing boundary respecting the theory of Novak et al, 1978. The Cylindrical model (or Cyl model) was first developed for the driving by Holeyman et al. (1984, 1996), further applied into vibratory driving by Vanden Berghe (2001) and extended to take the viscous soil reaction into account. The Cyl model allows the computing of the vertical displacements and the shear stresses induced in the soil into the far field due to the a dynamic pile solicitation.

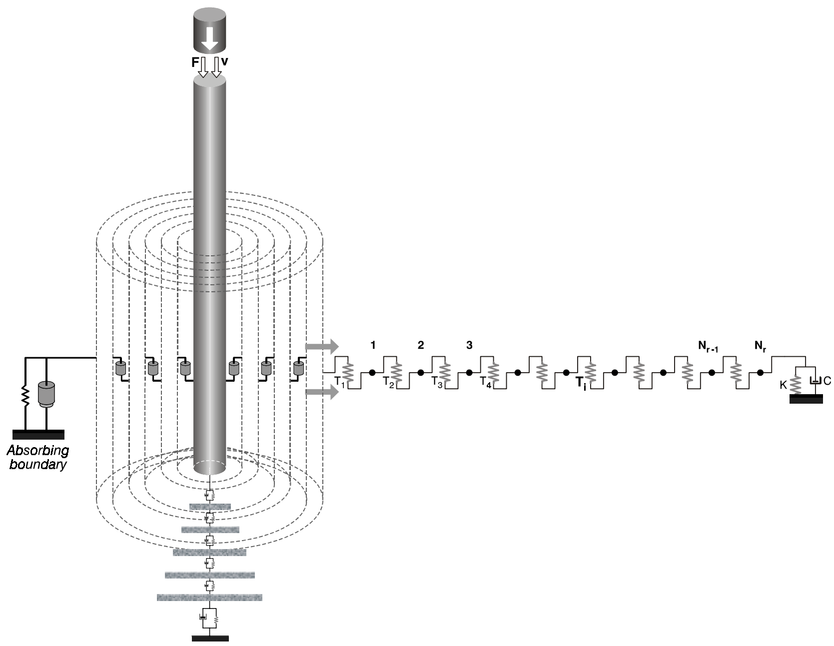

Figure V-2: Schematic view of the Cyl Model

Both models are focused on the shaft friction modelling and consider the pile as a rigid body influencing only one layer of soil. The pile imposes a vertical motion to the soil and according to the soil characterization, slippage occurs or not.

The models are solved with an explicit method. Accelerations are calculated based on the balance of the acting forces between media. These forces are computed (time t_i) with the displacement information of the preceding step (time t_{i-1}) (issued from the integration of the acceleration).

Both models were developed independently and some assumptions can be contradictory. Nevertheless, each approach brings conclusions that can be useful in the study of the influence of the loading rate.

2. The DDOF Model

2.1. Description

A new method has been developed in order to keep the advantages of the SDOF-model already presented in chapter 3 (time computing, simplicity, interest focused on the pile and of its direct vicinity and absence of reflecting waves) with the requirement to take into consideration slippage between the pile and the soil when the ultimate resistance is exceeded (required in chapter 4). This improvement only concerns the shaft friction and not the base soil reaction (not concerned by the slippage).

It must be possible to separate both medias, soil and pile, by considering their motions interdependently or not, without addition of a new horizontal element to the model. In other words, it is possible to take the soil motion into account at the close vicinity of the interface between pile and soil without modelling the soil up to a distance where it is not influenced by the pile motion.

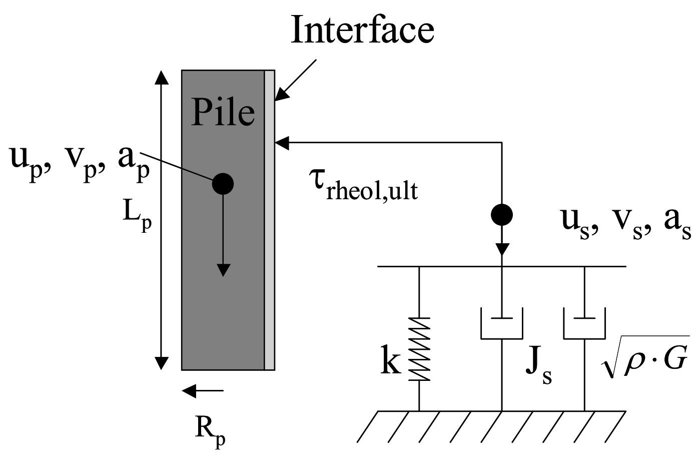

Figure V-3: Diagram of the new proposed shaft model

Nevertheless, without mass, there are some difficulties to estimate the independent motion of the soil when the slippage occurs. How to solve the equations of motion if the inertial term is eliminated or omitted? The proposed solution is based on the relation existing between the pile motion, the soil reaction and the ultimate value of the resistance acting at the interface of both medias (Figure V-3).

The pile moves according to its imposed motion and the balance with the external forces acting on itself. The soil follows this motion until the stress generated exceeds a variable threshold that determines the start of slippage and the uncoupling of both movements.

The soil reaction is represented by three terms. A spring, for the static behaviour, characterized by a hyperbolic stress-displacement relationship and a non linear stiffness k, a viscous dashpot representing the internal dissipation of energy, and a dashpot for the radiation term, characterized by a damping factor $\sqrt{\rho \cdot G}$. Those terms are already described in details in chapter 3 (Section 2.2.). The fundamental difference concerns the displacement and the velocity used in these formulations. Instead of the pile motion considered as unique and used previously, the soil motion is used (velocity and displacement). Since the motions are differentiated during slippage, the soil reaction is different than previously calculated.

$$\tau_s = \frac{\tau_{stat,ult}\left(1 + J_s \cdot v_s^{0.2}\right)}{\frac{u_r}{u_s} + 1}$$ the static and viscous terms **Equ. V-1**

$$\tau_{rad} = v_s \cdot \sqrt{G_i \cdot \rho} \cdot (1 - \eta)$$ the radiation term **Equ. V-2**

$$\tau_{rheol} = \tau_s + \tau_{rad}$$ **Equ. V-3**

$$\tau_{ult,rheol} = \tau_{stat,ult}\left(1 + J \cdot \left(v_p - v_s\right)^{0.2}\right)$$ the ultimate terms **Equ. V-4**

Where:

- $\tau_{stat,ult}$ is the ultimate static shear strength of the soil [MPa];
- τ_{stat} is the static soil reaction [MPa];
- J_s is the viscous damping factor [s/m$^{0.2}$];
- J is the rheologic damping factor [s/m$^{0.2}$];
- u_r is the quake [m];
- G_i is the initial shear modulus [MPa];
- η is the level of static mobilization: $\frac{\tau_{stat}}{\tau_{stat,ult}}$ [-];
- ρ is the soil mass density [kg/m^3];
- u_p, v_p is the pile displacement and velocity [m, m/s];
- u_s, v_s is the soil displacement and velocity [m, m/s].

The soil reaction is described by the sum of all terms until a limit determined by the slider limit (Equ. V-4). The slider represents the rheologic ultimate resistance of the soil under dynamic solicitations.

Both damping factors (J and J_s) are used equal to 0.5 s/m$^{0.2}$ but they represents different behaviours.

There is a fundamental change in the meaning of the ultimate resistance corresponding to the value of the plastic slider limit. The plastic slider is not a constant value nor dependent of the only pile velocity. The limit varies with the velocity differentiated at the pile/soil interface. This velocity is different from the soil velocity chosen to describe the viscous and the radiation terms. The interface velocity is nil until the starting of the slippage. This is a relative velocity, contrary to the pile or soil velocities which are absolute ones. The form of the equation is well known and generally used in the problems involved with loading rate effects.

The slider limit (the rheologic ultimate resistance) is equal to the ultimate static resistance (velocity independent) until a certain occurrence and becomes bigger and velocity dependent after this occurrence. The first limit, before the slippage occurs, is:

$$\tau_{rheol,ult} = \tau_{stat,ult} \qquad \textbf{Equ. V-5}$$

if $\tau_{rheol} \le \tau_{rheol,ult}$ **No slippage**

$$\tau_{rheol,ult} = \tau_{stat,ult} \cdot \left(1 + J \cdot \left(v_p - v_s\right)^{0.2}\right) \qquad \textbf{Equ. V-6}$$

if $\tau_{rheol} \ge \tau_{rheol,ult}$ **Slippage**

So, the threshold of soil resistance increases during the slippage with the interface velocity and the slippage starts when the resistance exceeds the static soil resistance. Before that, pile and soil, at the pile/soil interface, move with the same velocity, and are perfectly connected. When the slippage occurs, both behaviours start to diverge. The relative velocity (or interface velocity), (v_p - v_s), increases from zero to a certain value, positive of negative, defining the independent behaviour of both media. When the condition of Equ. V-6 is not achieved, both medias re-bond and v_p=v_s.

The slippage conditions are variable during the slippage but start and end with the same limit: $\tau_{stat,ult}$. It must be pointed out that the soil reaction is always velocity dependent, even if both pile and soil move coupled under the same solicitation. The rheologic stress is indeed function of two terms velocity dependent but linked to the soil motion: the viscous and the radiation terms.

The slippage is determined by the exceeding of a limit dependent of the interface velocity by a stress dependent of the soil velocity. The resolution of the problem is focused on the solving of v_s during the slippage event (u_p, v_p known – u_s, v_s unknown). The equilibrium of Equ. V-6 is used to obtain the value of v_s in an explicit scheme.

2.2. Algorithm

This algorithm describes the solving of v_s and u_s :

Equ. V-5 & Equ. V-6 are used:

When $\tau_{rheol} \le \tau_{rheol,ult} \rightarrow v_p = v_s$, $\tau_{rheol,ult} = \tau_{stat,ult}$ and $\tau_{rheol} = \tau_s + \tau_{rad}$

When $\tau_{rheol} \ge \tau_{rheol,ult} \rightarrow v_p \ge v_s$, $\tau_{rheol,ult} = \tau_{stat,ult} \cdot \left(1 + J \cdot \left(v_p - v_s\right)^{0.2}\right)$ and $\tau_{rheol} = \tau_s + \tau_{rad}$ and reduced to $\tau_{rheol} = \tau_{rheol,ult}$ so v_s and u_s are unknown.

The algorithm aims to find out v_s and u_s such as $\tau_{rheol} = \tau_s + \tau_{rad}$ = $\tau_{rheol,ult}$ = $\tau_{stat,ult} \cdot \left(1 + J \cdot \left(v_p - v_s\right)^{0.2}\right)$ during slippage.

Algorithm: calculation for t = t+ Δt

First time step after $\tau_{rheol} \geq \tau_{rheol,ult}$, v_p and u_p known.

Initial values: $v_s(t+\Delta t) = v_p(t+\Delta t)$

$$u_s(t+\Delta t) = u_s(t) + v_p(t+\Delta t)\cdot \Delta t$$

All the velocities and displacements expressed here below correspond to the time t+Δt.

1. Calculation of $\tau_{rheol} = \tau_s + \tau_{rad}$ (called **A**) with the initial values v_s and u_s;
2. Calculation of $\tau_{stat,ult} \cdot \left(1 + J \cdot (v_p - v_s)^{0.2}\right)$ (called **B**) with the initial values v_s and u_s;
3. Calculation of the difference **A-B = Δτ**;
4. Calculation $v_s^{*} = v_s - v_s \cdot \dfrac{\Delta\tau}{K}$;
5. Calculation of the corresponding displacement (u_s^{*}) and acceleration (a_s^{*}) for the proposed velocity (v^{*}_{s}) and using:

$u_s^{*}(t+\Delta t) = u_s(t) + \Delta t \cdot v_s^{*}(t+\Delta t)$ and $a_s^{*}(t+\Delta t) = \dfrac{v_s^{*}(t+\Delta t) - v_s(t)}{\Delta t}$

6. Test to validate the convergence criteria achievement $\left|v_s^{*} - v_s\right| \leq \varepsilon$;

Where ε is the required limit of convergence between two consecutive values of soil velocity (10^{-6} …10^{-8} m/s)

7. Interchanging of the corresponding values: $v_s = v_s^{*}$, $u_s = u_s^{*}$ and calculation of **A**: $\tau_{rheol} = \tau_s + \tau_{rad}$;
8. Loop of the points 2 to 7 until the convergence criteria is achieved;
9. a_s, v_s and u_s known for the time t+Δt and different of a_p, v_p and u_p.

The point 4. means that the closer the velocity to the solution, the smaller Δτ and so the increment.

The intermediate velocity v^{*}_{s} is a temporary one used to ensure the convergence in the algorithm.

It is possible to check the last solution for v_s with the Equ. V-7:

$$v_s = -\left[\left[\frac{1}{J}\cdot\left[\frac{(\tau_s + \tau_{rad})}{Q_{stat,ult}} - 1\right]\right]^{\frac{1}{0.2}} - v_p\right]$$

Equ. V-7

The algorithm is summarized on Figure V-4.

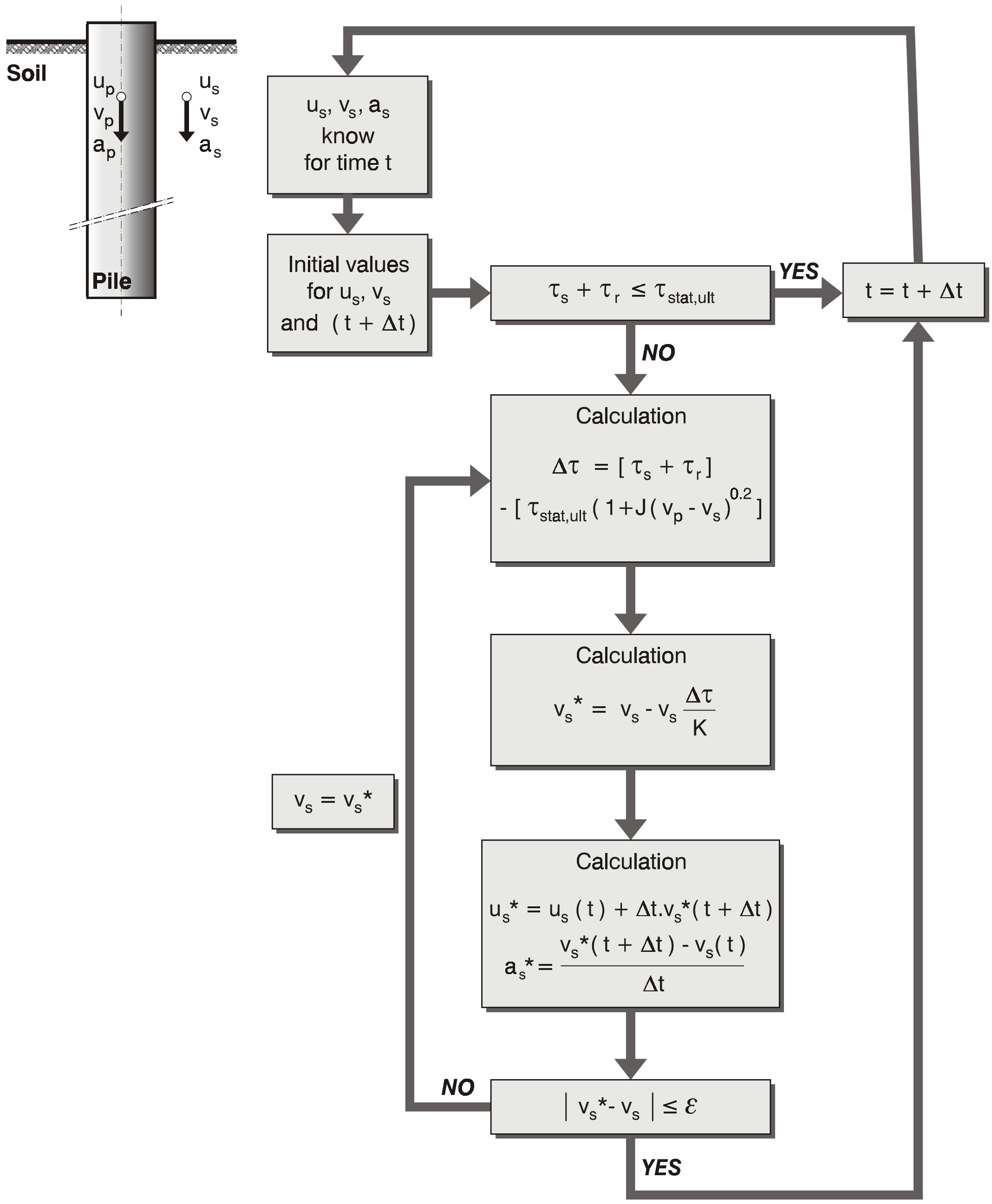

<u>Figure V-4</u>: algorithm of resolution for the DDOF model

The soil reaction during the slippage becomes:

$$\tau_{rheol} = \tau_s + \tau_{rad} = \tau_{stat,ult} \cdot \left(1 + J \cdot \left(v_p - v_s\right)^{0.2}\right) \qquad \textbf{Equ. V-8}$$

and allows to compute the pile motion for the next time step starting a new resolution loop of v_s .

The soil and pile re-bond when both velocities become equal ($v_p = v_s$) and when the soil reaction ($\tau_{rheol} = \tau_s + \tau_{rad}$) becomes inferior to the ultimate static resistance of the soil ($= \tau_{stat,ult}$).

The numerical convergence depends on the gap between **A** and **B** (points 3 & 4 of the algorithm). To ascertain this convergence, the constant K is introduced in order to smooth the variation imposed to v_s.

The value of K is set to 2…4 after a set of successful trials. The coefficient K has the same unit than $\Delta\tau$ so that the ratio $\frac{\Delta\tau}{K}$ is dimensionless.

The equations signs are significant to ensure the stability, the continuity and the convergence of the algorithm. The algorithm is relevant with the following rules:

If **A** $=(\tau_s + \tau_{rad}) > 0$ and $v_s > 0$ then

$$\tau_{stat,\,ult} > 0$$
$$\Delta\tau = \mathbf{A} - \mathbf{B} = (\tau_s + \tau_{rad}) - \tau_{stat,ult} \cdot \left(1 + J \cdot (v_p - v_s)^{0.2}\right)$$
$$v_s^* = v_s - v_s \cdot \frac{\Delta\tau}{K}$$

If **A** $=(\tau_s + \tau_{rad}) > 0$ and $v_s < 0$ then

$$\tau_{stat,\,ult} > 0$$
$$\Delta\tau = \mathbf{A} - \mathbf{B} = (\tau_s + \tau_{rad}) - \tau_{stat,ult} \cdot \left(1 + J \cdot (v_p - v_s)^{0.2}\right)$$
$$v_s^* = v_s + v_s \cdot \frac{\Delta\tau}{K}$$

If **A** $=(\tau_s + \tau_{rad}) < 0$ and $v_s < 0$ then

$$\tau_{stat,\,ult} < 0$$
$$\Delta\tau = \mathbf{A} - \mathbf{B} = (\tau_s + \tau_{rad}) - \tau_{stat,ult} \cdot \left(1 - J \cdot (v_p - v_s)^{0.2}\right)$$
$$v_s^* = v_s + v_s \cdot \frac{\Delta\tau}{K}$$

If **A** $=(\tau_s + \tau_{rad}) < 0$ and $v_s > 0$ then

$$\tau_{stat,\,ult} < 0$$
$$\Delta\tau = \mathbf{A} - \mathbf{B} = (\tau_s + \tau_{rad}) - \tau_{stat,ult} \cdot \left(1 + J \cdot (v_p - v_s)^{0.2}\right)$$
$$v_s^* = v_s - v_s \cdot \frac{\Delta\tau}{K}$$

The respect of this algorithm allows one to calculate the independent soil velocity without having to add a mass element to represent the soil in the close vicinity of the pile.

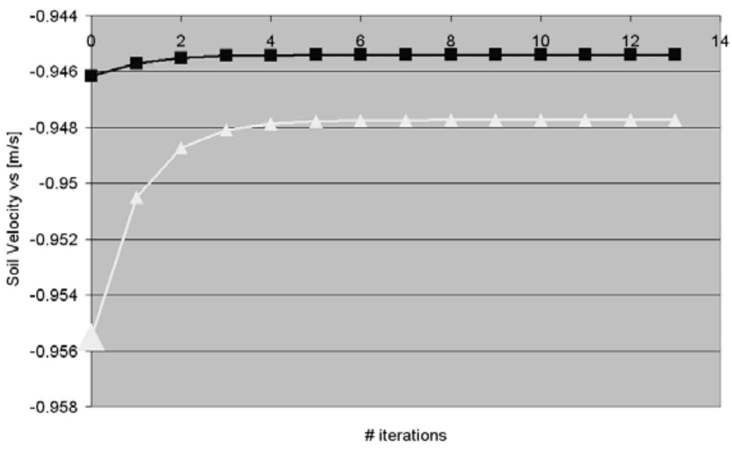

<u>Figure V-5</u>: Examples of v_s resolution

<u>Figure V-5</u> shows two examples of resolution by using this algorithm. As shown, the convergence is achieved quickly and stably. The biggest marks at the beginning of each curves show the initial values for v_s.

In order to use an implicit method, Equ. V-8 has to be simplified by gathering the terms in u_s and v_s. The problems could be solved using the Newmark integration scheme if the exponent N was set equal to 1 but not for N=0.2 as formulated.

After description of the algorithm, the results of simulations are presented in the following sections on a simplified model.

2.3. Simplified pile/soil model

This pile model only takes the shaft friction into account. The pile is geometrically characterized by a radius R and a length L. These two parameters are required to evaluate the static soil reaction (chapter 3, section 2.2.2 evaluation of the radius of influence R_m). A given synthetic motion is imposed to its head and transmitted to the soil. This motion is based on a real signal of velocity measured during a dynamic load test event. This modelling is described in details in chapter 3, section 2.4. and plotted in Figure V-6.

The velocity, the displacement and the acceleration signals are given by:

- $V(t)=V_o \cdot e^{(-\xi\omega t)} Sin(\omega t)$;
- $Acc(t)=\frac{\partial V(t)}{\partial t}=V_o \cdot \omega \cdot e^{(-\xi\omega t)}\left(-\xi \cdot Sin(\omega t)+Cos(\omega t)\right)$;
- $U(t)=\int V(t)dt=\frac{V_o}{-\xi\omega} \cdot \omega \cdot e^{(-\xi\omega t)} \frac{\left(Sin(\omega t)-\frac{\omega}{-\xi\omega}Cos(\omega t)\right)}{1+\frac{\omega^2}{(-\xi\omega)^2}}$.

Where ω is the circular frequency: 272 rad/s; V_0 is the initial velocity: 1.45 m/s and ξ is the attenuation coefficient: 0.233 rad^{-1}.

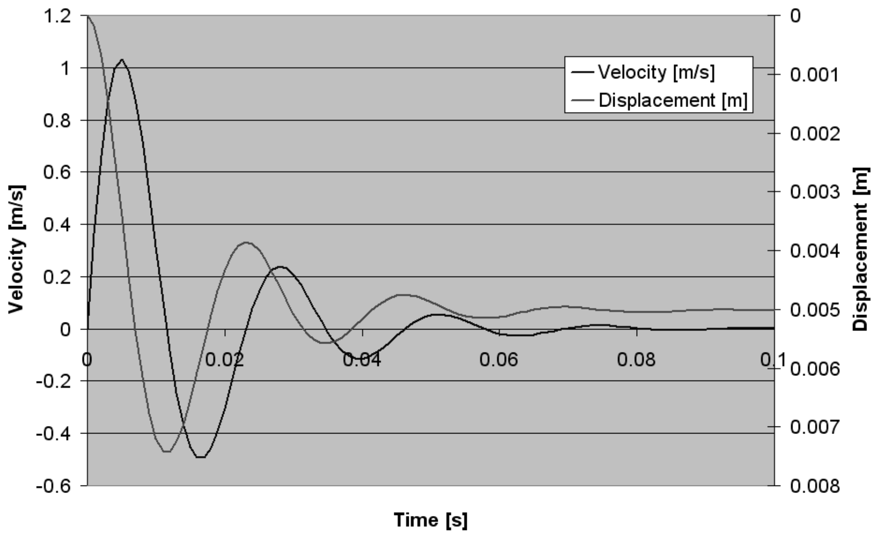

Figure V-6: Imposed motion (displacement and velocity)

The pile geometry parameters are given by:

- The pile length: 10 m;
- The pile radius: 0.2 m.

The pile is considered as rigid and the soil as one sole layer of which the characteristics are given by:

- Ultimate shear resistance $\tau_{stat,ult}$: 0.2 MPa;
- Poisson ratio υ: 0.35;
- Soil mass density ρ_{sol}: 2000 kg/m³;
- Initial shear modulus G_i: 100 MPa.
- Damping factor of the viscous term J_s : 0.5 s/m$^{0.2}$;
- Damping factor of the ultimate rheologic term J : 0.5 s/m$^{0.2}$;
- Velocity dependent power law exponent: 0.2.

The simplified model is described in Figure V-7 and called DDOF. A special attention is put to the interface behaviour (stress and motion).

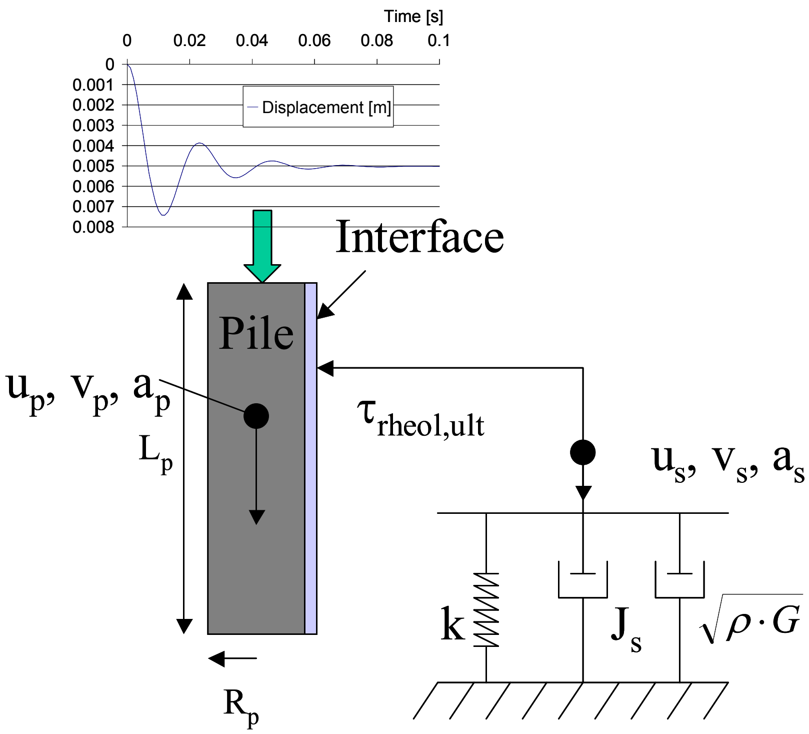

Figure V-7: description of the simplified pile/soil model

First, the results generated by this model are examined alone. After, a short analysis of the main parameters influencing the slippage or governing the interface velocity during slippage is proposed. Eventually, a comparison with the SDOF model, without slippage, in the same configuration, is performed.

2.4. Analysis of the DDOF Model results

Two sets of tests have been carried out to differentiate a case where the slippage is developed and a case where it is not. To allow this comparison, the static ultimate shear resistance $\tau_{ult,stat}$ is set to 0.2MPa and 2 MPa. The first soil resistance is too small and the second is sufficiently large to avoid the slippage. Those two cases allow the comparison with both typical behaviours concerned. The typical signals are pile and soil displacements; pile and soil velocities; interface soil reaction (static and rheologic) an the mobilization curves (soil reaction – soil/pile/interface displacement).

2.4.1 Comparison of the displacement curves

The first couple of figures (Figure V-8 et Figure V-9) show the displacement imposed to the pile (black trace), and the generated soil motion (white trace).

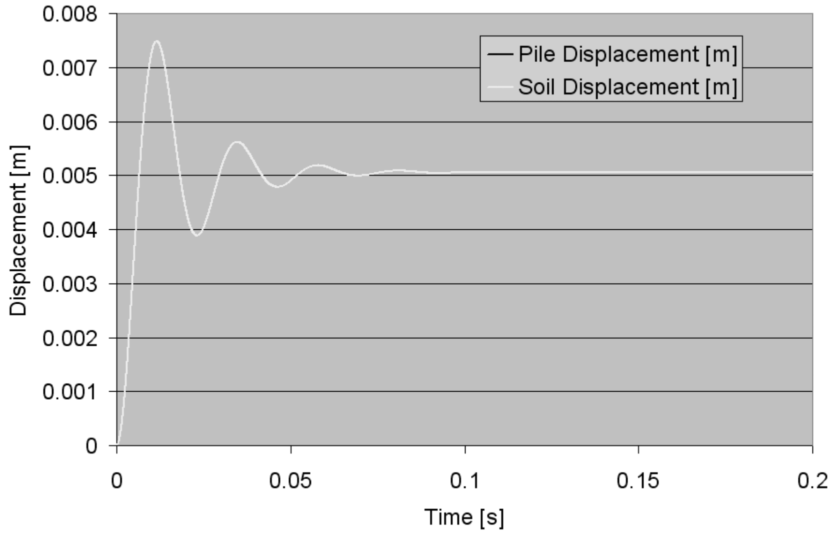

Figure V-8: Pile and soil displacements (DDOF model) - $\tau_{stat,\ ult}$: 2 MPa

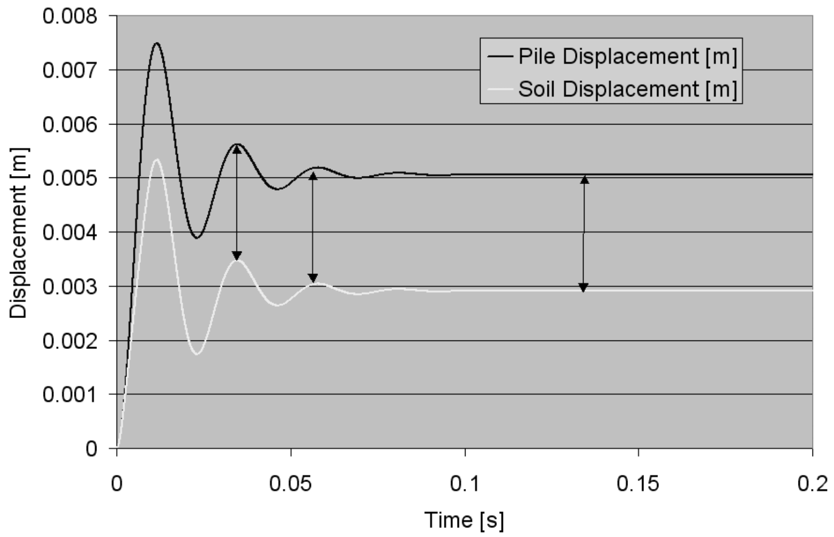

Figure V-9: Pile and soil displacements (DDOF model) - $\tau_{stat,\ ult}$: 0.2 MPa.

When the ultimate resistance is high enough, both elements, pile and soil, move coupled. Therefore, the displacement curves are superimposed (Figure V-8) and pile and soil in its direct vicinity undergo the same settlement path. On the other hand, the small strength threshold of the soil ($\tau_{stat,\ ult}$ = 0.2 MPa) influences directly the soil motion (Figure V-9). Both maximum and final displacements are influenced. The variation of displacement is working during the first part of the curve due to the strict period of slippage (differentiation of motion). After, both signals are perfectly parallel because the bodies are anew coupled (black arrows on Figure V-9). The difference of displacement is the effective penetration of the pile also called the permanent settlement.

2.4.2 Comparison of the velocity curves

Similarly to the displacement curves, when the ultimate resistance is too large, the pile and soil velocities are superimposed because they are continuously coupled (Figure V-10). Figure V-11 exhibits the result of the weakest soil. There are two occurrences of slippage during the first 30 ms.

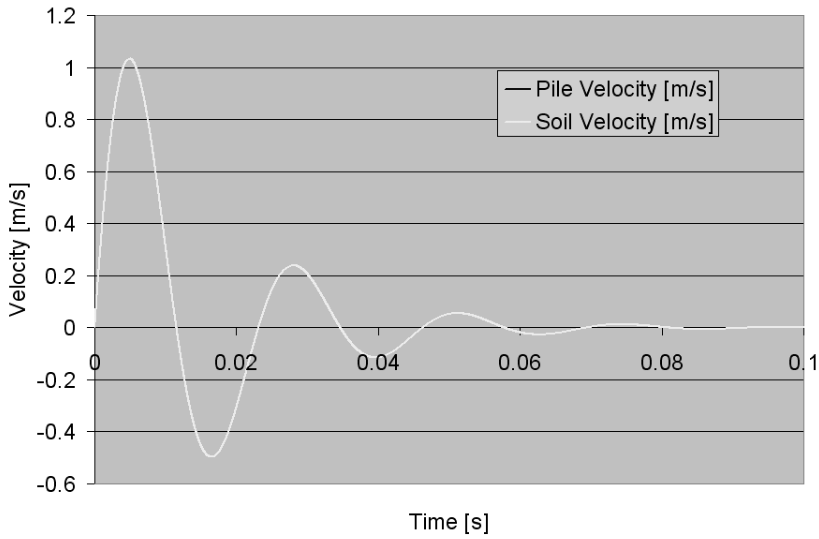

Figure V-10: Pile and soil velocities (DDOF model)- $\tau_{stat,\ ult}$: 2 MPa

The first slip event is clear and starts early in the motion evolution. The second is tiny and short and is barely visible on Figure V-11 (encircled).

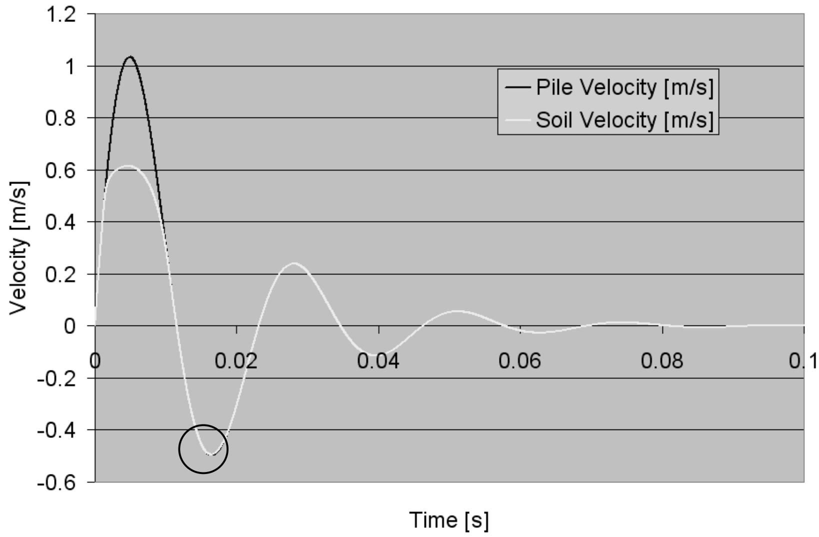

Figure V-11: Pile and soil velocities (DDOF model) – $\tau_{stat, ult}$: 0.2 MPa

The ultimate static resistance is exceeded twice during the simulation, once in the positive velocities field, once in the negative domain. Both modifications influence the soil and the pile behaviours. It is only during these periods that the pile settles down permanently compared to its direct vicinity. Figure V-12 is a zoom of the velocity curves focused where the velocities diverge. In order to have a better overview of the situation, this simulation has been performed with $\tau_{ult,stat}$ = 0.15 MPa highlighting a larger difference in the second slip occurrence. The light curve highlights the breaks in the continuity of the soil velocity history when the slippage starts and ends defining the passage to the failure mode and the slippage between the pile and the soil (two circles on Figure V-12).

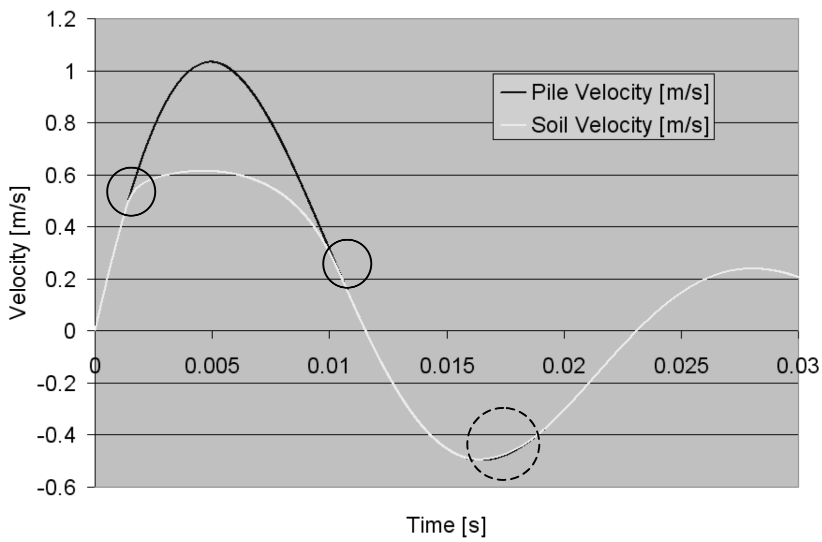

Figure V-12: Pile and soil velocities (DDOF model) – (zoom) $\tau_{stat, ult}$: 0.15 MPa

There is also a second break in the continuity of this trace (dashed circle on Figure V-12). During the second slip event, The first break point corresponds to the entrance in the failure mode. The second corresponds to the passage from positive static to negative static stresses. Since the soil velocity is nil when the static stress is maximum (arrow v_s =0 on Figure V-13), the velocity dependent term influence the stress "negatively". When the static stress crosses the zero level, all the terms of Equ. V-3 are of same sign and the evolution is similar to the first slip event. The point 1 corresponds to the passage to the failure mode while point 2. corresponds to the equalisation of the stress signs.

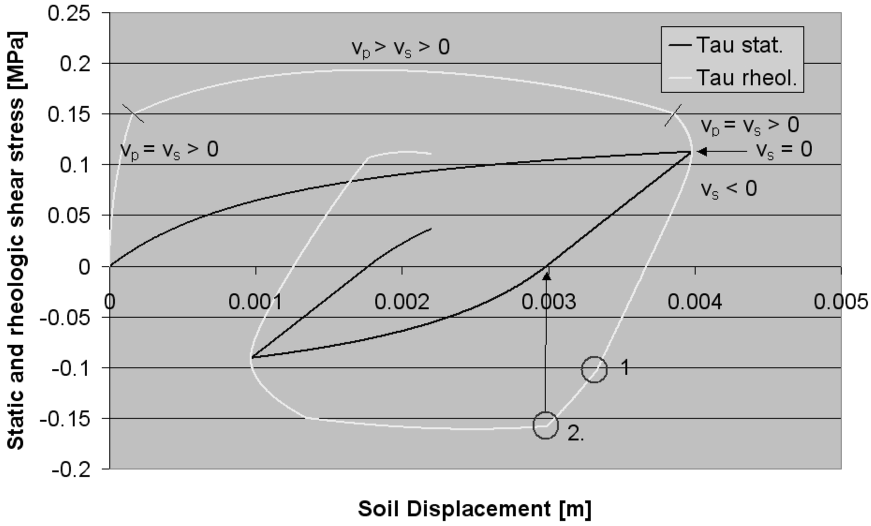

Figure V-13 : Static and rheologic shear stresses vs. soil displacement - $\tau_{stat, ult}$: 0.15 MPa

Figure V-14 exhibits the penetration velocity (v_p - v_s) in a simulation performed with $\tau_{stat, ult}$: 0.2 MPa. If this curve is integrated with respect to time, it wil result in the pile penetration. The differentiation of velocities (pile and soil) is similar to the Paquet approach (1988) (Figure V-15) wherein the interface velocity (v_p - v_s) is called the penetration or interface velocity. For Paquet, the final penetration of the pile (final gap between both displacement curves of Figure V-9) is connected to the penetration velocity. This differentiation of behaviours occurs when the slippage resistance is exceeded. The definitions of the limit and of the soil reaction are different but the methodology is similar.

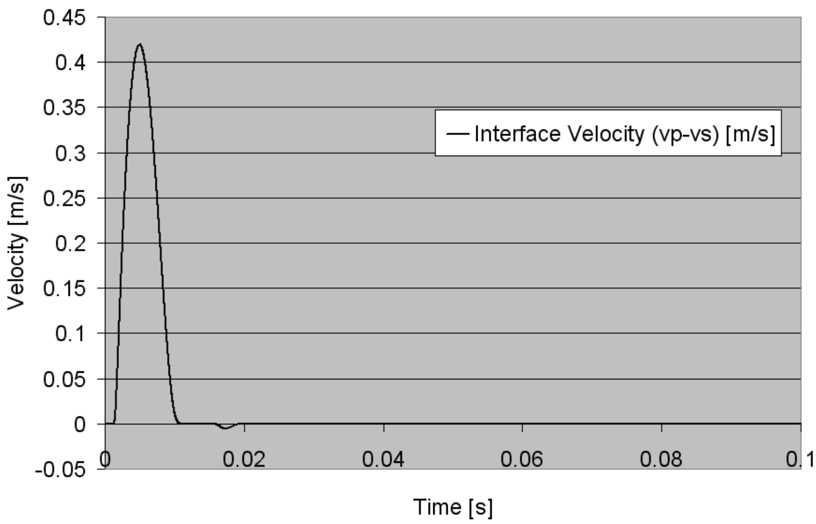

Figure V-14: Penetration velocity – $\tau_{stat, ult}$: 0.2 MPa

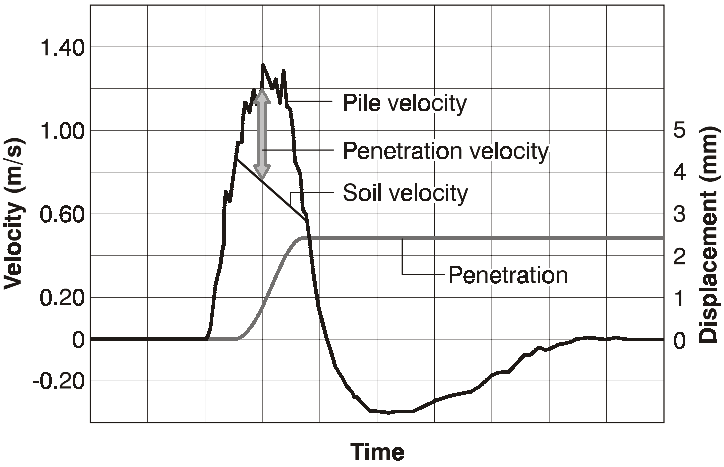

Figure V-15: Description of the Paquet model (Paquet, 1988)

Paquet challenges the classic formulation where the soil reaction is modelled by an elastoplastic soil reaction plus a viscous coefficient J (the rheologic term of the SDOF model). According to him, this approach seems to draw more upon empirical considerations than physical characteristics. There is no clear differentiation between the movement of the pile and the movement of the soil. The dashpot associated with the pile movement can not represent the radiative type damping (linked to the movement of the soil) or the viscosity of the penetration (associated with the difference of movement between the pile and the soil). Paquet states that the displacements of pile and soil are perfectly differentiated and their difference is the pile penetration. The reaction of the soil is represented by a spring and a dashpot theoretically determined by the expressions given by Briard (1970) and Novak et al (1978). They are linked to the soil displacement and represent the impedance of the soil layer (Figure V-16).

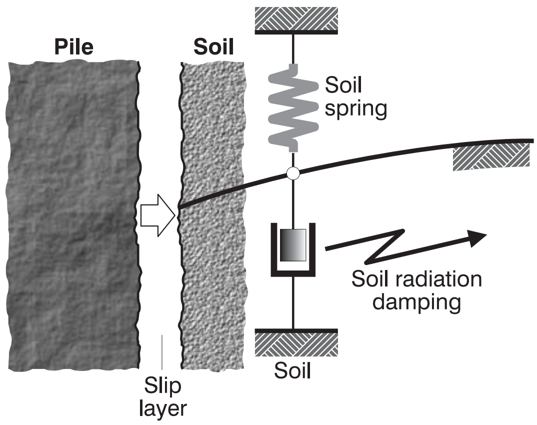

Figure V-16: Schematic Simbat model (Stain, 1992)

Heritier and Paquet have shown that the failure can be obtained from the stress generated by the radiative component (Heritier and Paquet, 1984). To take this failure into account, a slider is added to the Paquet's model to represent the possible slippage between the pile and the soil when the stress generated in the soil becomes larger than the limit. For Paquet, this limit can be a function of the mean penetration velocity or the static ultimate resistance associated with a dashpot. This approach is particularly similar to the approach explained in this section.

2.4.3 Comparison of the static and rheologic stress curves

The static and rheologic stresses can also be examined. The static stresses (related to the non linear spring via hyperbolic relationship) and the rheologic stresses (sum of all terms: static, viscous and radiative) are differentiated on Figure V-17 and Figure V-18 . These terms are linked to the soil motion (velocity and displacement). Since the ultimate soil resistance is large enough to avoid slippage in Figure V-17, the static stress curve looks like the displacement trace (even though the stiffness is not linear and decreases with the soil mobilization).

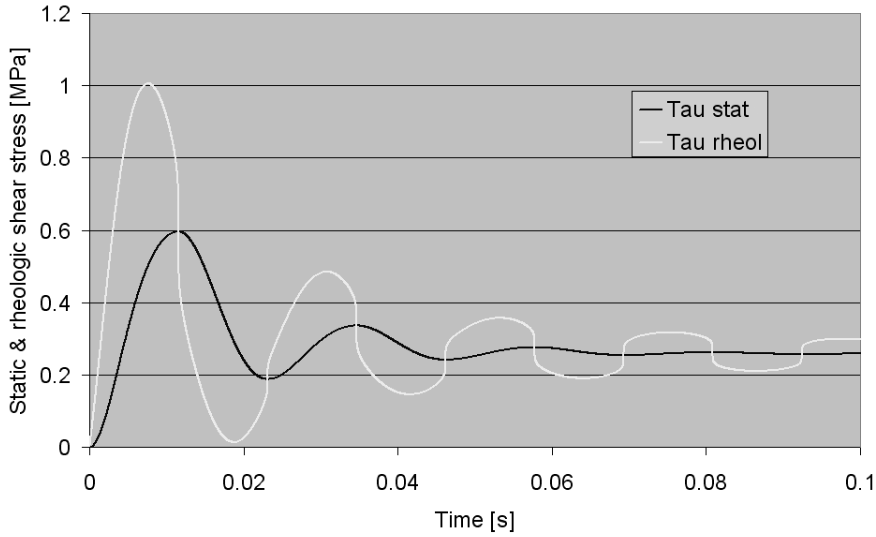

Figure V-17: Rheologic and static stresses (DDOF model)- $\tau_{stat, ult}$: 2 MPa

Both rheologic and static traces are characterized by a same frequency and a phase gap. Since the velocity is ahead of the displacement (Figure V-6), this influence is recovered in the displacement and velocity dependent terms of the rheologic stress. Figure V-18 highlights the influence of the slippage on the static stress. The soil motion is eased and the level of reached stresses is highly reduced (as expected). Figure V-18 is still itemized with the addition of the trace of the difference between the rheologic and the static stress traces (Figure V-19). The result exhibits the influence of the soil velocity and the predominance of the velocity dependent terms in the rheologic stress evaluation, especially in the beginning of the mobilization.

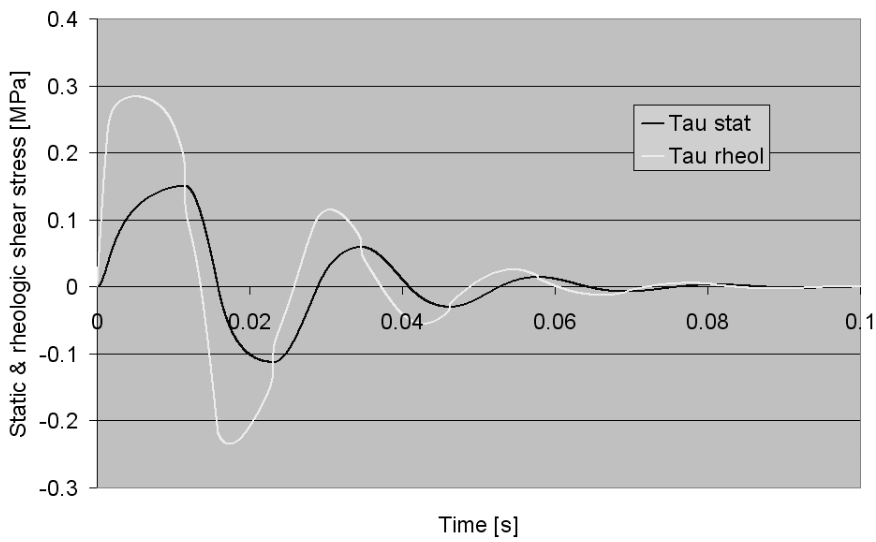

Figure V-18: Rheologic and static stresses (DDOF model)- $\tau_{stat, ult}$: 0.2 MPa

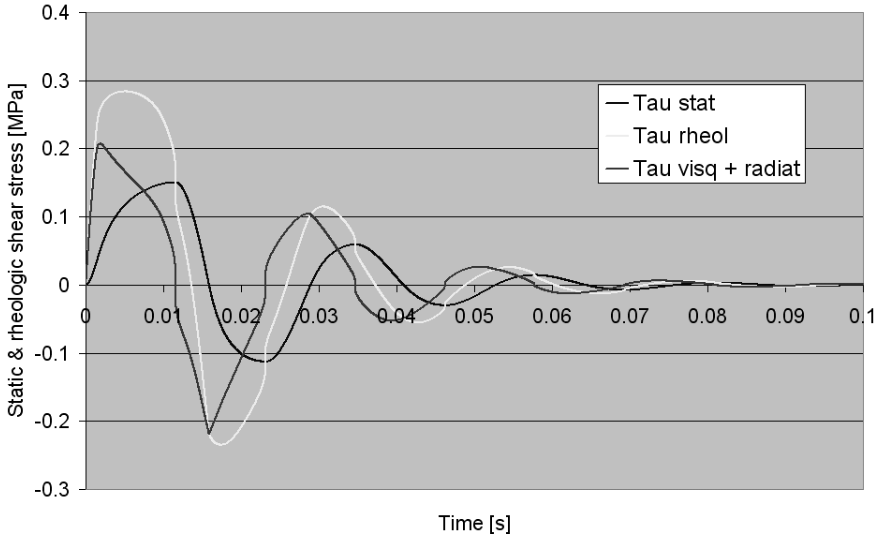

Figure V-19: Rheologic, static stresses and their difference (DDOF model)- $\tau_{stat,\,ult}$: 0.2 MPa

The final stress state of the soil is function of the soil reaction history and of the ultimate stress level of soil resistance. For a same motion imposed, if the first simulation ($\tau_{ult,stat}$ = 2 MPa) results in a certain state of residual stress along the pile shaft (about 0.26 MPa), the second proposition ($\tau_{ult,stat}$: 0.2 MPa) almost nullifies the final stresses around the pile. This parameter influences the final stress state of the pile/soil interaction (influence in the static equilibrium and the dynamic analysis during driving).

2.4.4 Comparison of the displacement-stress curves

The static behaviour of both simulations (τ_{ult} = 0.2 MPa and τ_{ult} =2 MPa) remains hyperbolic (Figure V-20 and Figure V-21) and the influence of the velocity dependent terms is greatly influenced by the sign of the soil velocity.

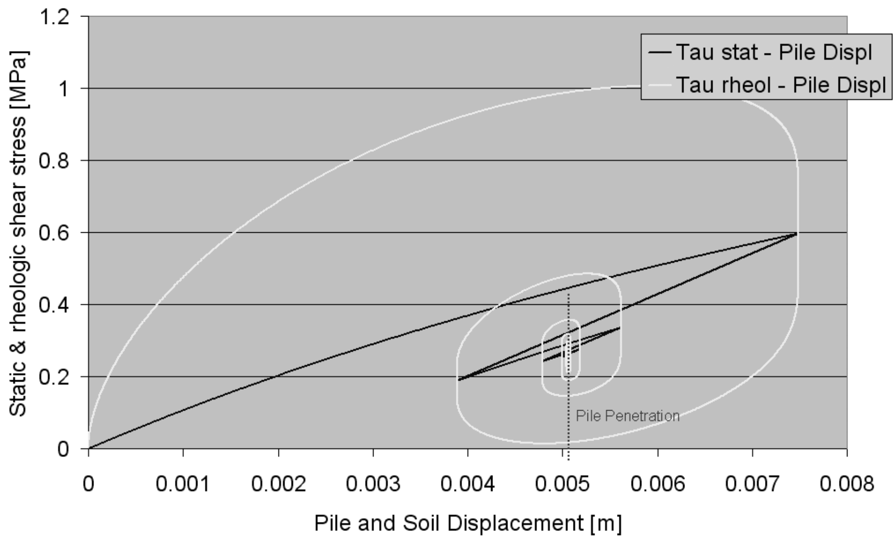

Figure V-20: Static and rheologic stresses vs. pile & soil displacements - $\tau_{stat,\,ult}$: 2 MPa

Figure V-20 shows the case without slippage ($\tau_{ult,stat}$: 2 MPa). The pile and soil displacements are coupled all the time and the four traces are superimposed two by two. The pile penetration is nil compared to the adjacent soil because both displacements are coupled but is equal to its final position compared to the initial referential.

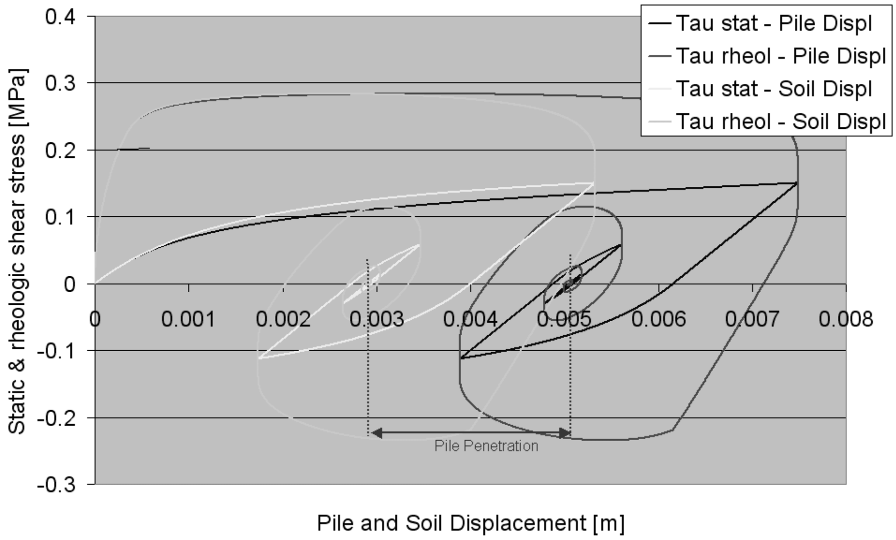

Figure V-21: Static and rheologic stresses vs. pile & soil displacements - $\tau_{stat,\ ult}$: 0.2 MPa

Figure V-21 exhibits the behaviour of the soil reaction with respect to the pile and the soil motions. The difference between both final settlements can be considered as the net settlement of the pile sliding into the soil. Nevertheless, compared to the initial referential, the final position of the pile is the final settlement. there is a settlement of the soil in the direct vicinity of the pile influenced by the pile motion. Since the final displacement is different, the settlement path does not influence the unloading parameters optimisation and the ratio of shear modulus G_2/G_i could be fixed to 1 without influence on the optimisation of the other parameters (to be checked with complete model). The first part of the traces is identical for both displacements because both behaviours are coupled at this moment and are only differentiated during the slippage. This slippage occurs for a rheologic stress superior to $\tau_{stat,ult} =$ 0.2 MPa as expected.

2.5. Influence of a variation of $\tau_{ult,stat}$

This section compares the evolution of the main curves already described (displacement, velocity, rheologic stress) for a variation of ultimate static soil resistances (from $\tau_{ult,stat}$: 0.02 MPa to 0.7 MPa). The parameters of the pile/soil system remain the same than listed in section 2.3. The response of the pile/soil system with $\tau_{stat,ult}$: 0.7 MPa corresponds to a situation where no slippage occurs (identical to case $\tau_{stat,ult}$: 2 MPa presented previously).

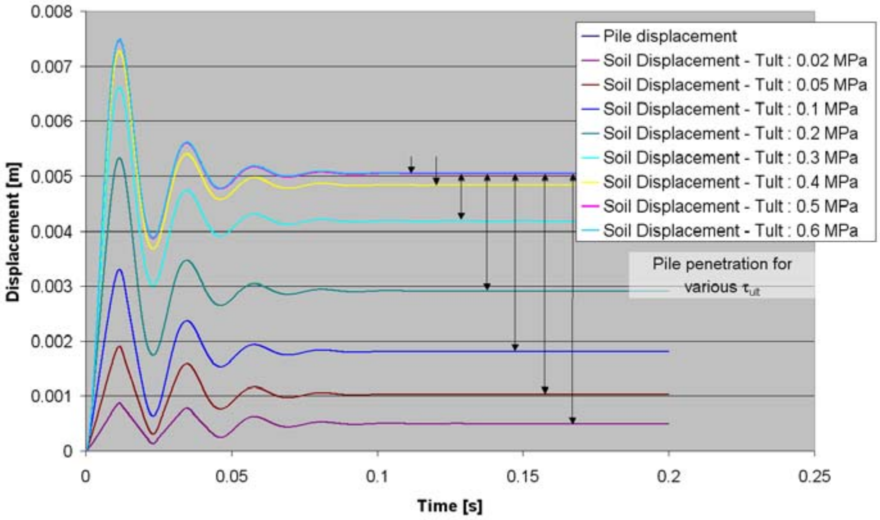

Figure V-22: Pile and soil displacements (DDOF model) - $\tau_{stat, ult}$: 0.02 to 0.7 MPa

Figure V-22 exhibits the traces of the generated soil displacement for each case of ultimate static shear stress proposed. The evolution is similar to the stress trend. The maximum soil displacement reached increases with $\tau_{stat,ult}$ like the final settlement of the soil. On the other hand, the pile penetration (u_p-u_s) (Figure V-23) decreases with $\tau_{stat,ult}$.

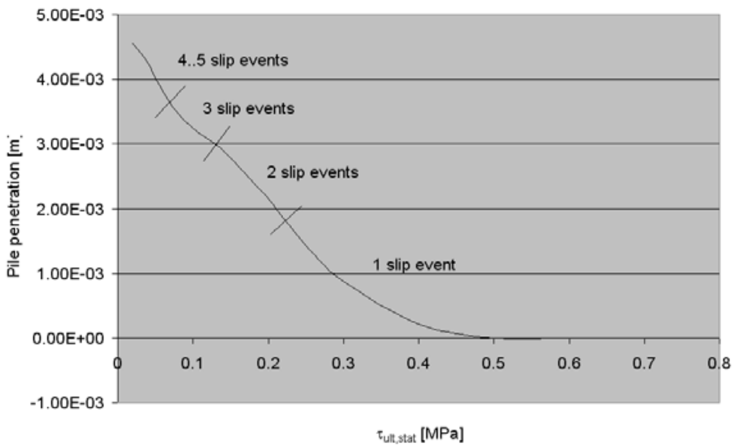

Figure V-23: Evolution of the pile penetration in the DDOF model for various τ_{ult}

The evolution of the pile penetration with $\tau_{ult,stat}$ depends on the number of slippage events and their timing. If the slippage occurs when the velocity is positive, the reduction of the soil velocity compared to the pile velocity results in an increase of the final pile penetration. If the opposite situation is observed (slippage occurring during a period where velocities are negative), the consequence is a decrease of the pile penetration. This is illustrated by the evolution of the curve of Figure V-23 where the progression of the pile penetration is slowed down when two slippage events (the first in positive velocities and the second in negative velocities) perturb the pile/soil system response.

As expected, the number of slippage events increases when $\tau_{ult,stat}$ decreases because the threshold of resistance to be exceeded to enable slippage decreases.

Figure V-24 shows the evolution of the soil velocity compared to the pile velocity for the same variation of $\tau_{ult,stat}$.

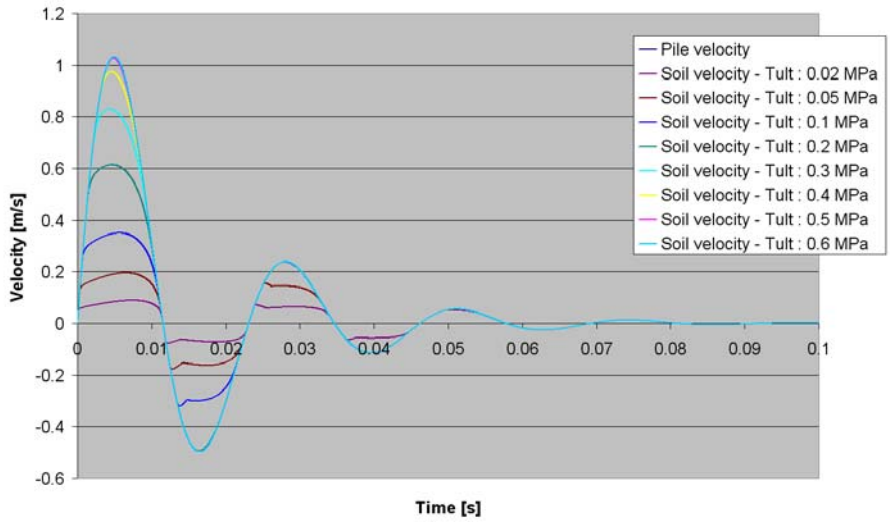

Figure V-24 : Pile and soil velocities (DDOF model) - $\tau_{stat,\ ult}$: 0.02 to 0.7 MPa

Figure V-24 exhibits the strong influence of the ultimate static resistance in the evaluation of the soil velocity with the proposed model. When the ultimate static resistance is reduced, the disconnections start more and more early and the number of slip events increases. If the soil resistance is very poor, the soil motion is greatly influenced and the corresponding soil velocity and displacement are very small for a same imposed pile motion. The pile and soil velocities remain of the same sign during the separations. There is a re-bonding before each change of velocity sign. The larger the ultimate resistance, the more similar the velocity curve compared to the pile one.

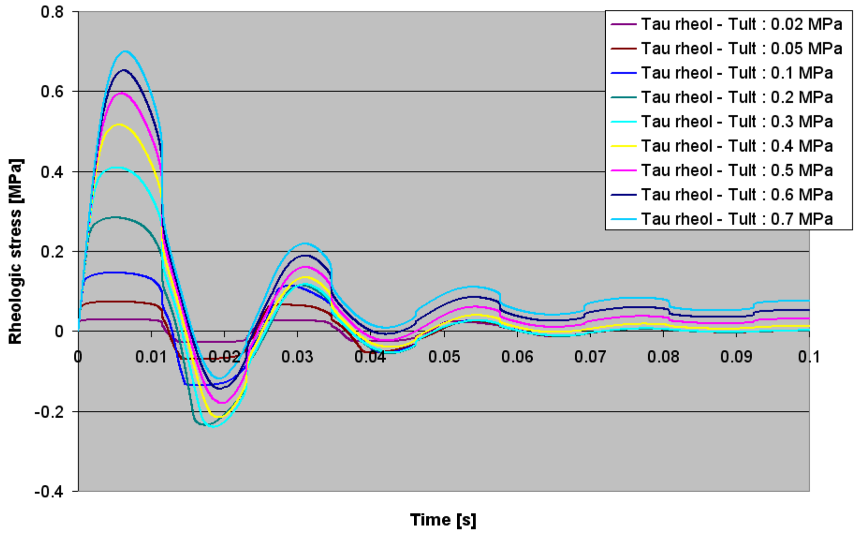

Figure V-25: Rheologic stresses (DDOF model) - $\tau_{stat,\ ult}$: 0.02 to 0.7 MPa

Figure V-25 describes the evolution of the rheologic stresses for a variation of ultimate static strength. The change of ultimate static stress influences more the peak value than the final state of the rheologic stress. The first peak illustrates this link because of the complete mobilization of the resistance and the development of the slippage resistance (dependent of the interface velocity). The final shear stress state remains approximately in the same range due to the small levels of velocities.

2.6. Influence of a variation of the rheologic parameter J

The pile/soil system response is defined by the equations Equ. V-1 to Equ. V-4. In those equations, besides the ultimate static stress, other parameters are of importance: the rheologic parameters J and N. Since N is fixed in the literature, it is interesting to evaluate the influence of J on the slippage development. The following figures summarize this analysis with the traces of the main quantities already presented in the previous sections: the soil displacement and velocity and the rheologic stress with respect to time compared to the pile motion. J is proposed varying between 0.1 and 5 (s/m). Both damping factors (J and J_s) are used equal but they represents different behaviours. The first is linked to the soil (viscous one, J_s) and to its velocity (v_s), and the second is a failure parameter linked to the interface behaviour (J).

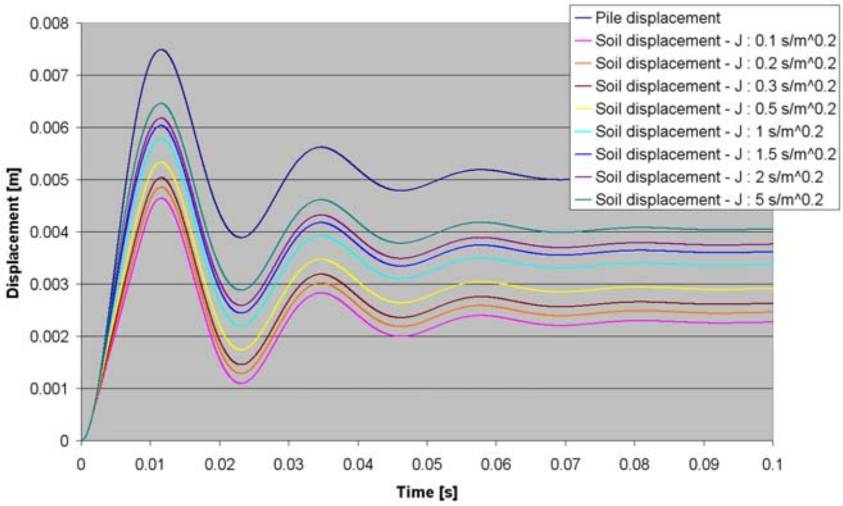

<u>Figure V-26</u>: Evolution of the soil displacement curves with variation of J - $\tau_{stat,\ ult}$: 0.2 MPa

<u>Figure V-26</u> displays the soil displacement traces for each proposed value of J. The influence of J on the whole trace is very important. It is slightly more pronounced on the final displacement (about 2mm). The parameter J has a great influence on the soil displacement and the slippage development.

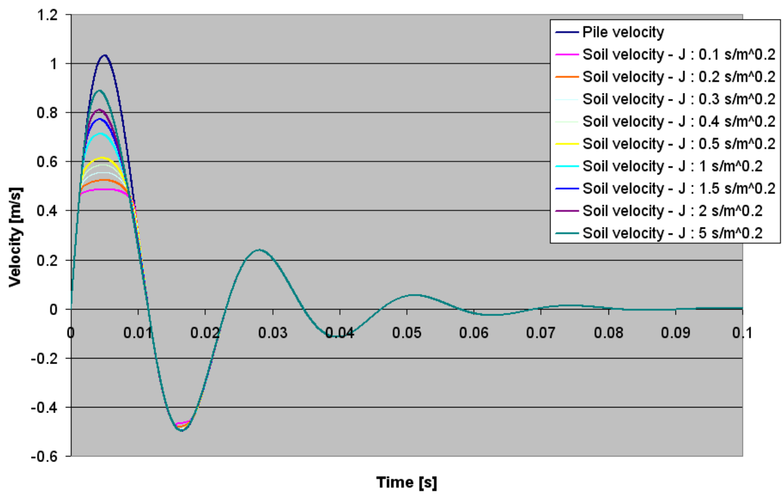

<u>Figure V-27</u>: Evolution of the soil velocity curves with variation of J - $\tau_{stat,\ ult}$: 0.2 MPa

Figure V-27 exhibits the evolution of the generated soil velocity for the variation of J. The influence is very important especially in the first peak of velocity. The soil velocity can vary from 0.5 m/s to more than 0.9 m/s under the selected variation of J. Moreover, the smaller the damping factor, the more sudden the starting of the slippage; the larger the parameter J, the smoother the evolution of the soil velocity during the passage from soil mobilization to failure (there is no breaking in the continuity when both curves separate and re-bond). It can be pointed out that the higher the damping factor, the smaller the penetration velocity (v_p-v_s) with a direct influence on the number of slippage occurrences. Only 5 simulations (J from 0.1 to 0.5 s/m$^{0.2}$) cause a second slip event.

The same value is used for the viscous soil parameter J_s and for the interface parameter J (Equ. V-1 and Equ. V-4). Since they represent two different behaviours, their values must be different but in order to limit the number of parameters to be variable, this research has been performed with the same value.

Figure V-28 exhibits the rheologic stress traces. The increases of the parameter J results in an increases of the soil velocity (viscous term and radiation term) and a reduction of the penetration velocity (ultimate rheologic stress). Consequently, the higher the parameter J, the more accentuated the influence of the velocity dependent terms on the rheologic stress. The viscous term is also highly influenced by the increase of J (see the trace corresponding to J= 5 s/m$^{0.2}$). When the velocity (pile or soil) becomes almost null, the effects of the variation of J tend to vanish.

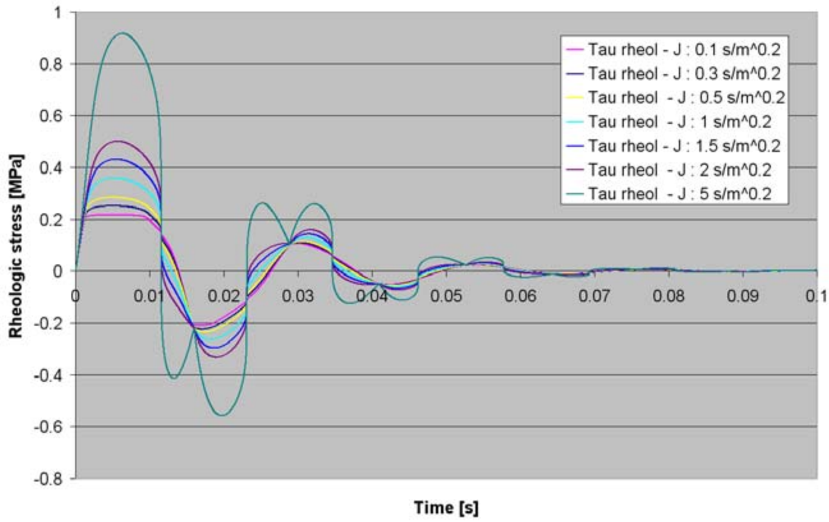

Figure V-28: Evolution of the rheologic stress curves with variation of J – $\tau_{stat, ult}$: 0.2 MPa

2.7. Influence of the differentiation of J and J_s

Equ. V-1 and Equ. V-4 illustrate the loading rate effect by the introduction of the velocity dependent terms. The first expression describes the viscous effect and the second is supposed to illustrate the evolution of the ultimate soil resistance with the soil velocity. Both expressions use a same approach with a power law of the velocity (absolute or relative) multiplied by a constant value (J and J_s). The values of J and J_s were always used equal due to a lack of information of the viscous damping factor and due to the reduction of the number of parameters, this common value is generally fixed to $0.5 s/m^{0.2}$. However, the behaviours described are completely different: the viscous damping J_s is linked to the soil and to the absolute soil velocity v_s while the rheologic damping factor J is linked to the interface velocity only acting during slippage (v_p-v_s).

This section presents the case where the slippage is forced and where both parameters J and J_s are taken into account with a specific value.

- $J = 0.5\ s/m^{0.2}$ as usual;
- $J_s = 0.05\ s/m^{0.2}$.

The following figures (Figure V-29 to Figure V-32) present the evolutions of the displacement, velocity and stress curves of this new situation compared to the usual one with $J=J_s$.

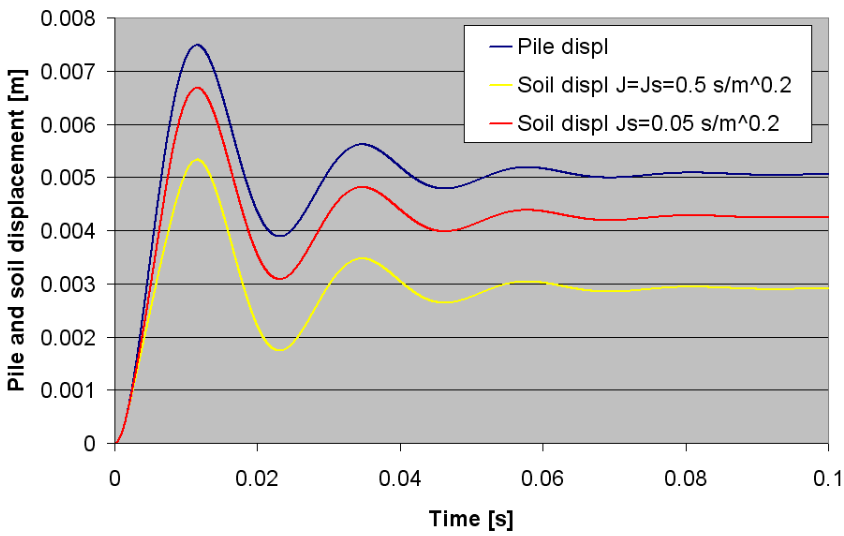

Figure V-29 : Evolution of the soil displacement curves - $\tau_{stat, ult}$: 0.2 MPa

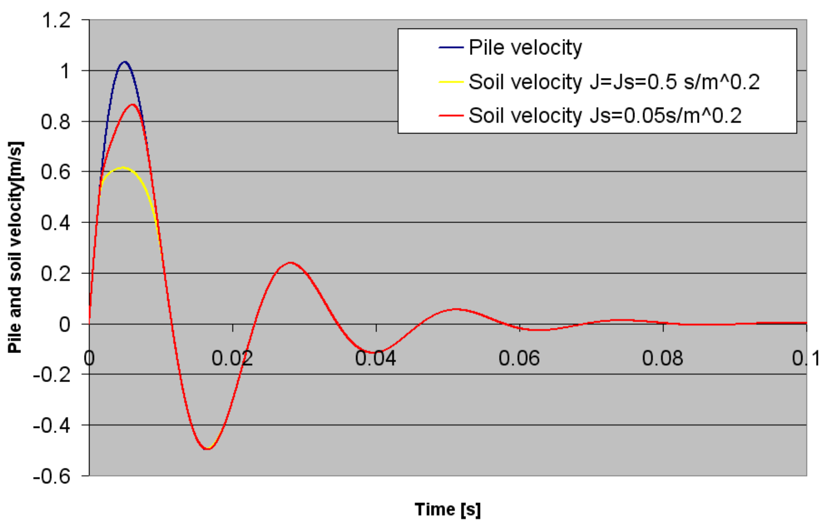

Figure V-30 : Evolution of the soil velocity curves - $\tau_{stat, ult}$: 0.2 MPa

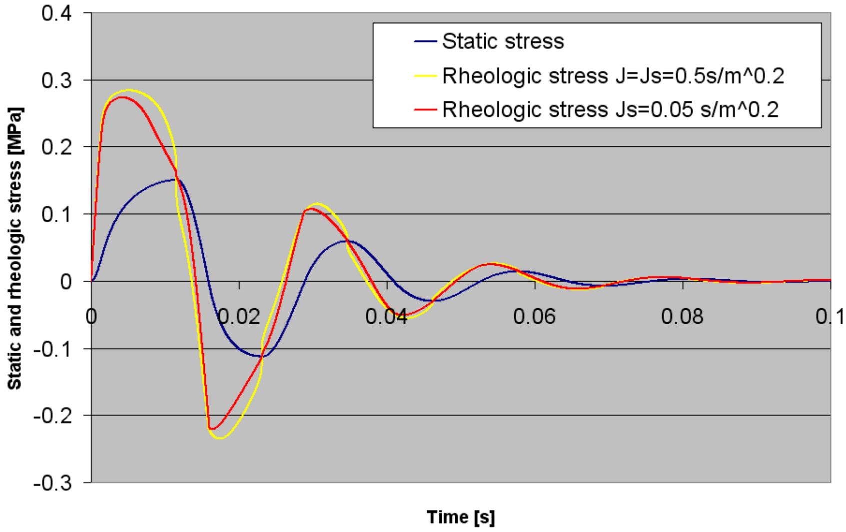

Figure V-31 : Evolution of the static and rheologic stress curves - $\tau_{stat,\ ult}$: 0.2 MPa

The slippage consequences are highly reduced with this change but not suppressed. This highlights the relative importance of the viscous term in the rheologic formulation. The soil velocity (Figure V-30) generated during the slippage in order to equilibrate the slippage condition (Equ. V-6) is larger than for the case $J=J_s$, the penetration velocity is then smaller; the soil displacement is also more developed and the pile penetration is decreased (Figure V-29). The static stress is exactly the same as expected, and the rheologic stress history does not evolve significantly (Figure V-31).

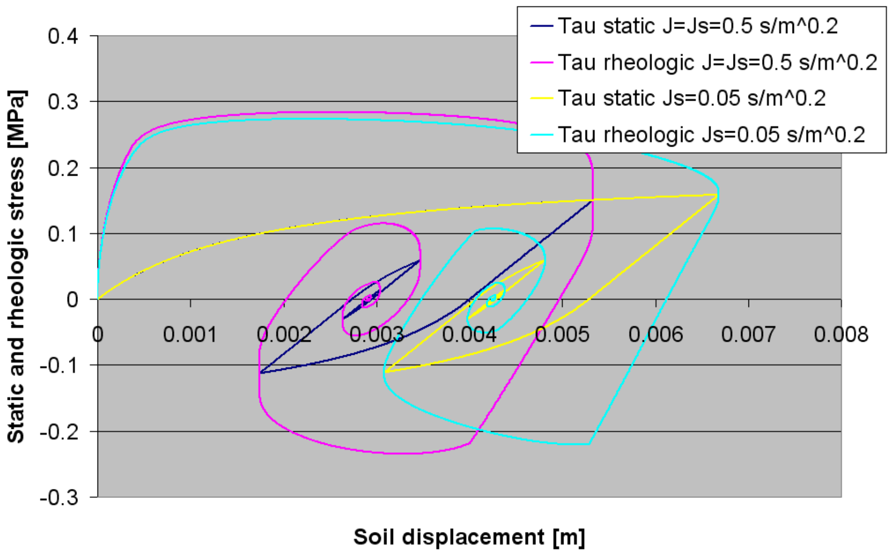

Figure V-32 : Static and rheologic stresses vs. pile & soil displacements with J & J_s different - $\tau_{stat,\ ult}$: 0.2 MPa

Since the soil motion is influenced by the differentiation of J and J_s (larger soil displacement and velocity), the stress-soil displacement relationships take these modifications of behaviour into account. The new traces (J different from J_s) are in an intermediate position between both traces related to the pile and soil motions (for $J=J_s$).

Other parameters can be studied with a particular influence on some terms of the rheologic stress. For example, the importance of the radiation term is highlighted by the influence of the variation of G_i in the generation of the slippage. Since the ultimate stress is quickly saturated if the shear modulus is increased, the slippage of both media is also influenced by the variation of this parameter.

2.8. Comparison with the SDOF model

After this description of the result of the DDOF model submitted to an imposed motion, it can be interesting to compare the responses of the DDOF model with the SDOF model under the same imposed motion and pile/soil system. The comparison is illustrated by the soil mobilization (reaction and motion). The pile and the soil are herefore described with the same parameters:

- Poisson ratio = 0.35;
- G_i = 100 Mpa;
- ρ_{sol} = 2000 kg/m³;
- Pile radius = 0.2 m;
- Pile length = 10 m;
- τ_{ult} = 2 MPa and 0.2 MPa;
- J: undifferentiated damping parameter = 0.5 s/m$^{0.2}$;
- Relative velocity exponent = 0.2.

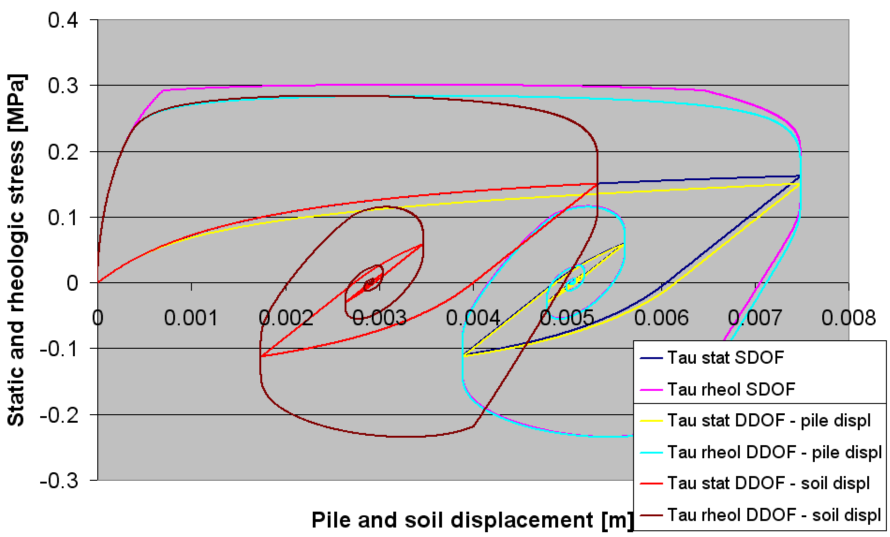

Figure V-33: Comparison of the static and rheologic stresses vs. pile and soil displacement for the models SDOF and DDOF – $\tau_{stat, ult}$: 0.2 MPa

Figure V-33 describes the stress-displacement relationships relevant for both models (SDOF and DDOF) and for the combinations soil reaction – pile and soil displacements (especially for the DDOF model). The simulations are proposed with slippage development.

Since the pile motion is imposed, the displacement histories corresponding to the pile motion (sole case for the SDOF model, one of both cases for the DDOF model) are identical. The differentiation comes from the stress evaluation.

Before the slippage happens, all the curves are superimposed (static and rheologic). After, the DDOF traces disassociate according to the pile and soil motions. The SDOF static stress history respects the DDOF soil static stress history aspect and not the pile one. This is due to the DDOF model which follows the soil motion instead of the pile motion. The development of the hyperbolic curve (stress-displacement relationship) is lead by the soil motion.

The rheologic stress histories exhibit the differentiation in the formulation of the velocity dependency. The SDOF expression is linked to the absolute pile velocity and the DDOF relationship uses the interface velocity which is activated during the slip event.

The passage from the description of the soil reaction to the failure mode is also different (marked by a discontinuity in the traces). Since the starting of the slippage is determined by the exceeding of the ultimate static shear strength in the DDOF model and of a velocity dependent formulation of this limit for the SDOF model, they cannot be similar:

$$\tau_{ult,rheol} = \tau_{ult,stat}\left(1 + J \cdot v_p^{0.2}\right)$$ **Equ. IV-36**

$$\tau_{ult,rheol} = \tau_{ult,stat}\left(1 + J \cdot \left(v_p - v_s\right)^{0.2}\right)$$ **Equ. V-4**

Consequently, since the pile is authorized to slip and the soil-displacement relationship allowed to be interrupted during this slippage, the final position of the displacement to be respected at the end of the unloading phase is inferior in the DDOF model. The influence on the back-analysis (see chapter 4) and in the optimisation procedure should be less significant.

The logical next step is to implement this model on a complete pile/soil model including more soil layers, a pile modelled in different elements, the base reaction represented by the equivalent soil cone and to perform the back-analysis process on real measurements of a dynamic load test. Unfortunately, this was not possible in the framework of this research by lack of time, but it remains certainly a major requirement for the future of this work.

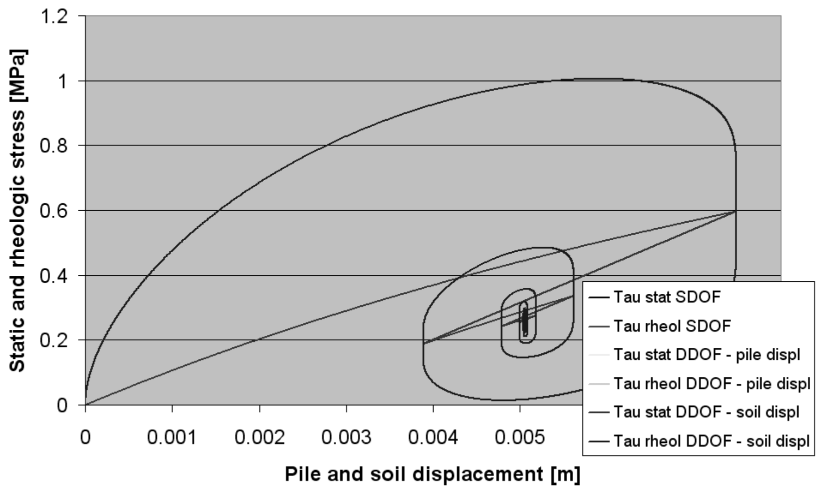

Figure V-34: Comparison of the static and rheologic stresses vs. pile and soil displacement for the models SDOF and DDOF – $\tau_{stat,\ ult}$: 2 MPa

Figure V-34 displays the same traces than in Figure V-33 but in a situation where the ultimate static stress is never exceeded. Consequently, there is no slippage. Figure V-34 confirms that in this case, both models are equivalent and all curves are superimposed (for the static and rheologic aspects).

3. The Cylindrical Model

The model described hereafter, called the Cylindrical model (Cyl model), allows one to figure the soil behaviour submitted to an excitation generated by a dynamic loaded pile. This behaviour is described in the close vicinity of the pile and farther in order to investigate the attenuation of the wave propagation into the soil. The model is firstly described, with the geometrical and algorithmic aspects. After, it is validated and the study is finally focused on the slippage between the pile and the soil and its propagation into the soil.

3.1. Description

The geometric description of this model (pile/soil system) uses a cylindrical symmetry. The soil is assumed to be a disk of which the thickness increases slightly and linearly with the distance from the centre of the pile (also the axis of the symmetry) as suggested by Holeyman (1984) (Figure V-35).

The increase of thickness is a linear function of the radius and tends to simulate the radiation damping provided by the vertical diffusion of waves around the moving pile. Equ. V-9 represents this relationship:

$$\Delta h = \alpha \cdot \Delta r \qquad \textbf{Equ. V-9}$$

where:

- Δh is the increase of thickness per unit of distance from the centre of the disk [m];
- Δr is the thickness of each cylinder [m];

- α is the coefficient of dispersion that quantifies radiation into the half-space underlying the pile base level (= 0.03 – Holeyman (2000)).

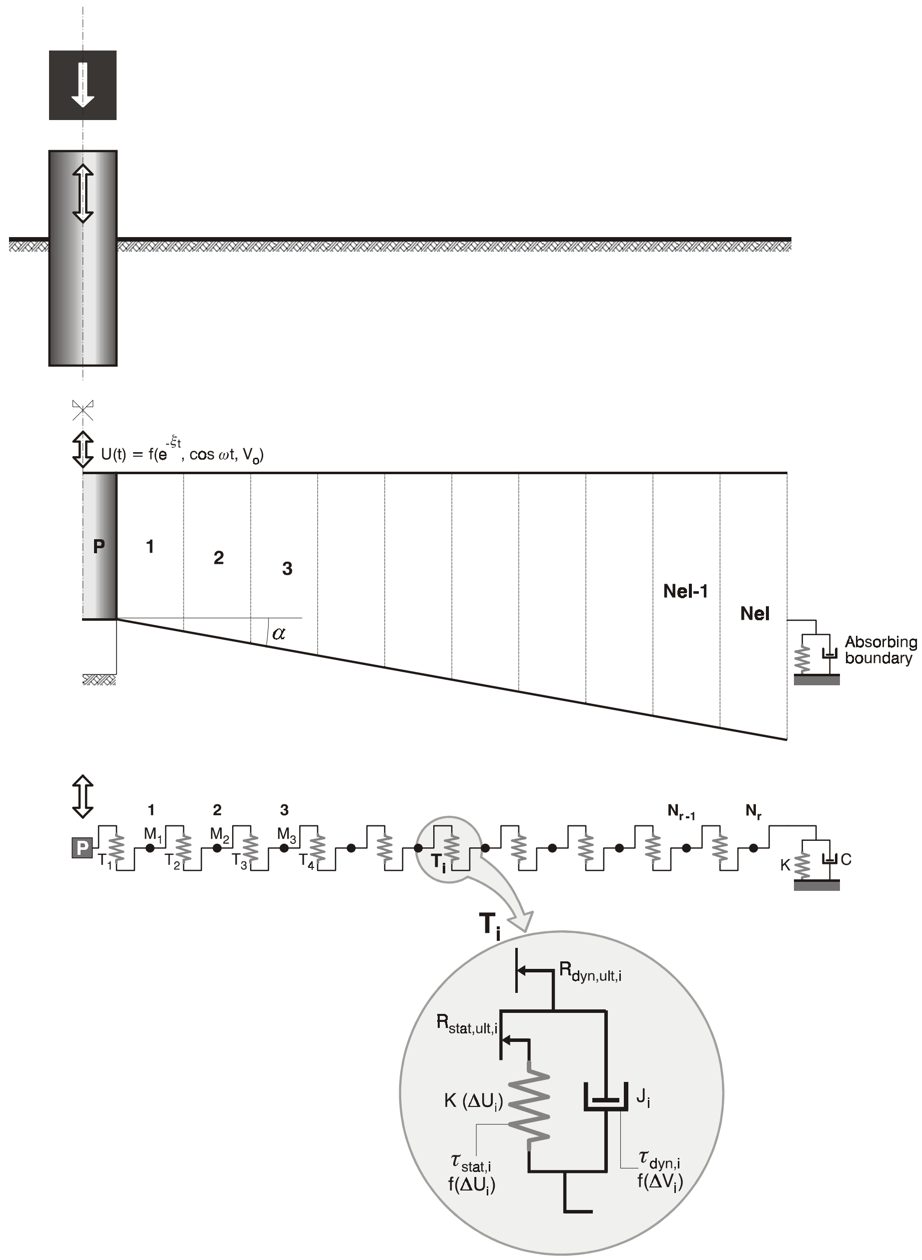

Figure V-35: Geometric model (based on Holeyman, 1984)

For the SDOF model, the radiation damping is taken into account through a linearly velocity dependent formulation called the geometric damping:

$$\tau_{geom} = \sqrt{\rho \cdot G} \cdot v \qquad \textbf{Equ. V-10}$$

where:

- ρ is the soil volumetric mass [kg/m³];
- G is the instant tangent shear modulus [MPa];
- v is the soil velocity [m/s].

The disk of soil is discretized in a set of concentric rings characterized by a mass and the same width. Each element transmits forces acting to its boundaries to the adjacent elements. The base resistance of each element is supposed to balance gravity (Vanden Berghe, 2001).

The vertical shear stress at the interface between two rings is computed based on the relative displacement of them and a corresponding stress-displacement relationship.

The loading rate effect is taken into account by a viscous term and the ultimate rheologic soil resistance. Both of them are velocity dependent. The viscous effect and the slippage condition are related to the interface velocity (or the relative velocity between two adjacent soil elements).

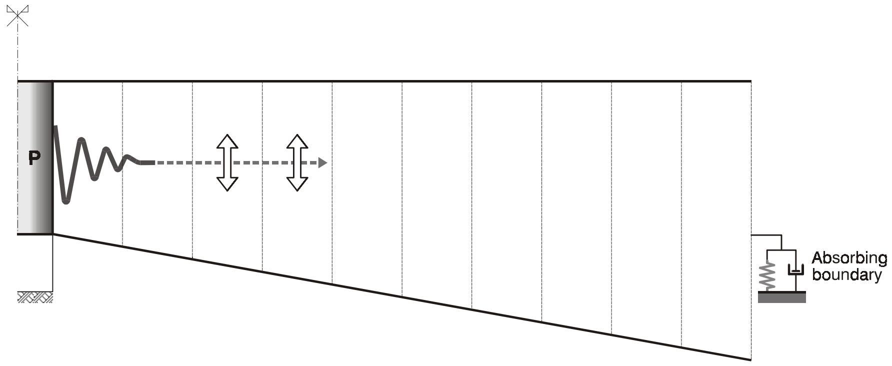

Figure V-36: Geometric propagation and interactions with the soil elements

The radial discretization is characterized by the number of rings (N_{el}), the thickness of each element (Δr) and the length of the pile (L) for the masses and surfaces (Figure V-36). The last element of the model must have a boundary condition. This border is built in a such way that the direct waves arriving from the pile are absorbed by this border (Novak et al., 1978).

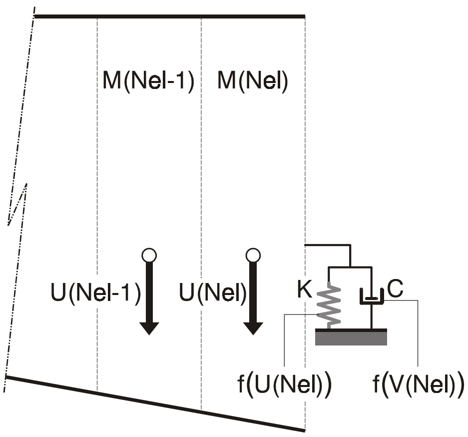

Figure V-37: Schematic description of the outer boundary of the Cyl model

This element is described in chapter 2. It is developed for a plane strain solution of soil displacement under harmonic solicitation for an infinitely long massless and rigid cylinder vibrating in an infinite elastic, homogeneous and isotropic medium (Novak et al. (1978)).

The model boundary is given by:

$$k = 2\pi G_s \frac{a_0^* K_1\left(a_0^*\right)}{K_0\left(a_0^*\right)}$$ **Equ. II-69**

- $a_0 = \frac{\omega r_0}{V_s}$ is the dimensionless frequency of the cyclic motion;
- r_0 is the pile radius;
- $a_0^* = i a_0$ with i the imaginary unit $i = \sqrt{-1}$;
- ω is the circular frequency;
- V_s is the shear wave velocity of the soil;
- $K_{0,1}$ is the modified Bessel function of the second kind of order 0 and 1 respectively.

That could be rewritten as:

$$k = G_s\left(S_{v1} + iS_{v2}\right) = K + iK'$$ **Equ. II-70**

The boundary element can be approximated by a spring and a dashpot of which the constants are frequency independent and defined by:

$$K = G_s \cdot S_{v1} \text{ [N/m/m']}$$ **Equ. II-71**

$$c = \frac{G_s r_0}{V_s} S_{v2}\left(a_0 = 1\right)) \text{ [N.s/m/m']}$$ **Equ. II-72**

The units of K and c correspond to the unit of length of the vibrating cylinder (the pile in this case) Novak et al., (1978).

The model simulates the infinite medium but according to the assumptions of Novak's theory, the waves are absorbed only if the stresses generated remain in the elastic domain. To fulfil this condition, the number of soil elements and the distance of the border from the pile must be large enough to ensure that the wave is damped sufficiently at the boundary (Holeyman et al, 1994).

3.2. Algorithm

Similarly to the previous section dedicated to the DDOF model and the slippage problem, a certain motion is imposed to the pile and the pile/soil and the soil/soil responses are described and commented with a special interest to the slippage occurrence. The descriptions of the pile and of the imposed motion are proposed in Section 2.3. of this chapter.

The forces acting on each soil element and on the pile shaft are summarized on Figure V-38 and Figure V-39 and are linked to a single cylindrical soil element (section view in Figure V-38).

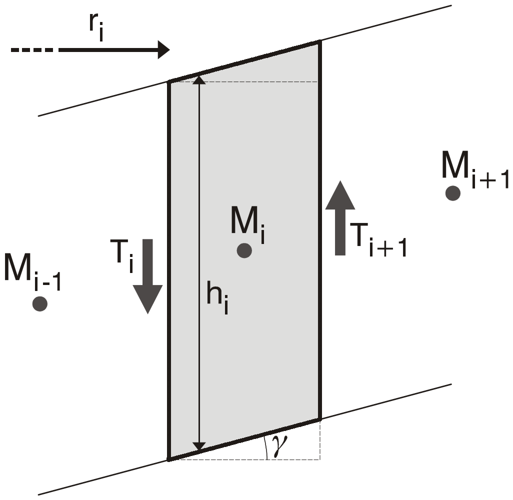

Figure V-38: Forces acting on soil elements (after Vanden Berghe, 2001)

The inter-ring reaction is calculated assuming an uniform distribution of the shear stress along the internal and external shaft of the soil element.

$$T_i = 2\pi \cdot r_i \cdot h_i \cdot \tau_i \qquad \textbf{Equ. V-11}$$

where:

- T_i is the inter-ring reaction between elements i and i-1;
- r_i is the radius of the interface between elements i and i-1;
- h_i is the average height of elements i and i-1;
- τ_i is the shear stress at the interface between elements i and i-1;
- γ is the angular distortion of the soil element caused by the resulting acting force;
- M_i is the mass of element i.

Based on the reactions acting at the interface between elements, the acceleration $acc_i(t)$ of the soil element i is calculated by:

$$acc_i(t) = \frac{(T_i - T_{i+1})}{M_i} \qquad \textbf{Equ. V-12}$$

where:

- $acc_i(t)$ is the acceleration of element i;
- T_i is the inter ring reaction between elements i and i-1;
- T_{i+1} is the inter ring reaction between elements i+1 and i.

In the same way, the stress at each interface is based on the relative displacement of the two concerned soil elements. This relative displacement is linked to the stress through the angular distortion:

$$\gamma = \frac{u_{i-1} - u_i}{\Delta r} \qquad \textbf{Equ. V-13}$$

where:

- u_i & u_{i-1} are the displacement of elements i and i-1;
- Δr is the additional radius between the positions of both soil elements.

The first interface stress, in contact with the pile, gets a shear strain influenced by the pile and the soil motions. Since the pile is rigid, the distortion is calculated only on the first soil element. The distance of reference becomes the thickness of the element reduced by half:

$$\gamma = \frac{2(u_{i-1} - u_i)}{\Delta r}$$ **Equ. V-14**

The previous relation has a limited domain of validity, because the approximation agrees with the real deformation only if Δr is small enough to replace the tangent approximation by its argument ($tg(\theta) \cong \theta$ only if θ is small). Consequently, the soil element has to be small enough to ensure the algorithm precision and the numerical stability.

The resulting stress is calculated based on the distortion γ and one of the following classic stress-strain relationships:

- Pure elastic relationship;
- Elasto-plastic relationship;
- Hyperbolic relationship.

These relationships are defined in Chapter 3 in the section dedicated to the SDOF model and the shaft friction.

Classically, the loading rate effect is taken into account by a viscous stress contribution and by the definition of the ultimate rheologic shear resistance, both terms being velocity dependent. The viscous term and the ultimate rheologic shear stress are evaluated from the interface velocity (the relative velocity between elements).

The velocity of each element is obtained from the acceleration by simple time integration:

$$vel_i(t + \Delta t) = vel_i(t) + acc_i(t + \Delta t)\Delta t$$ **Equ. V-15**

where:

- $vel_i(t)$ and $vel_i(t+\Delta t)$ are the velocities of element i at the time t and at the next time increment.

The loading rate effects affect the soil resistance by increasing the static term of the soil reaction by a velocity dependent term. The Gibson and Coyle (1968) proposed power law is used to account of this behaviour:

$$\tau_{rheol,ult} = \tau_{stat,ult} \cdot \left(1 + J \cdot (v_i - v_{i-1})^{0.2}\right)$$ **Equ. V-16**

$$\& \ \tau_{rheol} = \tau_{stat} \cdot \left(1 + J_s \cdot (v_i - v_{i-1})^{0.2}\right)$$

where:

- τ_{rheol} and $\tau_{rheol,ult}$ are respectively the rheologic soil reaction and the ultimate rheologic resistance;

- τ_{stat} and $\tau_{stat,ult}$ are respectively the static soil reaction and ultimate static resistance;

- J_s and J are the damping factors defining the load rate effect for the viscous and the ultimate behaviours, respectively.

The general algorithm becomes:

- The pile is moving in function of a predetermined motion;

- This motion implies the resolution of the forces balance at the interfaces between elements (in particular between the pile and the first soil ring);

- From this equilibrium, the acceleration, the velocity and the displacement of each element are generated;

- Time is incremented to next step and process is re-iterated.

Figure V-39 summarises the different steps of the process for a full time increment.

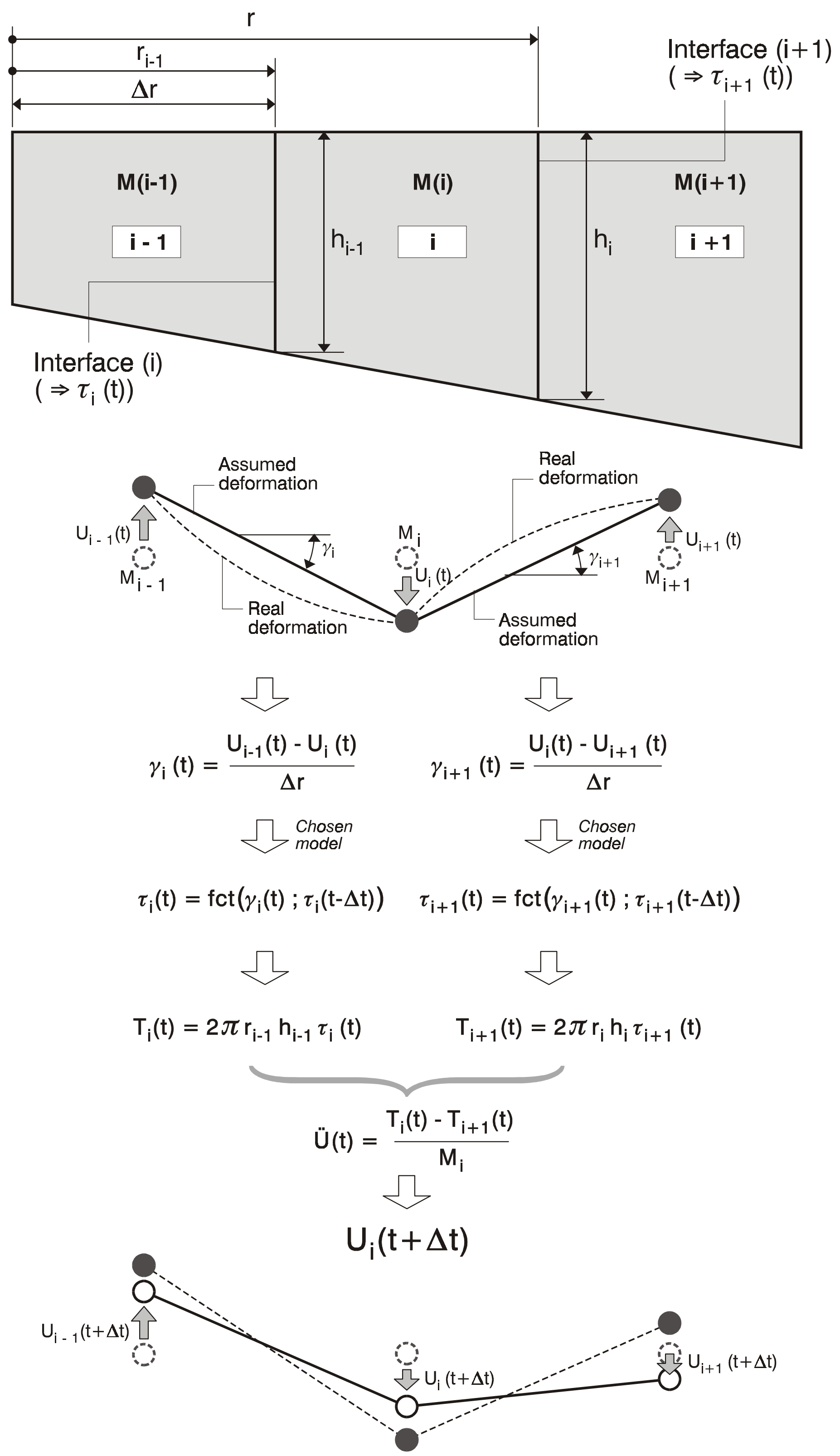

<u>Figure V-39</u>: Summary of the displacement of the soil element i at the time step t+Δt (after Vanden Berghe, 2001)

The axial symmetry of the model could be described with the complete stress state in a cylindrical coordinates system (r,θ,z) (<u>Figure V-40</u>).

In an axially symmetric distribution of stresses the non-vanishing components are σ_r, σ_θ, σ_z and τ_{rz}. The non-vanishing velocity components are u and w, respectively perpendicular and parallel to the Z axis. The velocity-component in the circumferential direction v is equal to zero since the flow is confined to meridian planes. The stresses and velocities are independent of θ and are only functions of r, z and time (i.e. $\partial(..)/\partial\theta = 0$).

The soil is assumed to be fully saturated. The dynamic event is supposed to be short enough to avoid the excess pore water dissipation during the dynamic load test. Therefore, the model considers the behaviour of the soil as undrained.

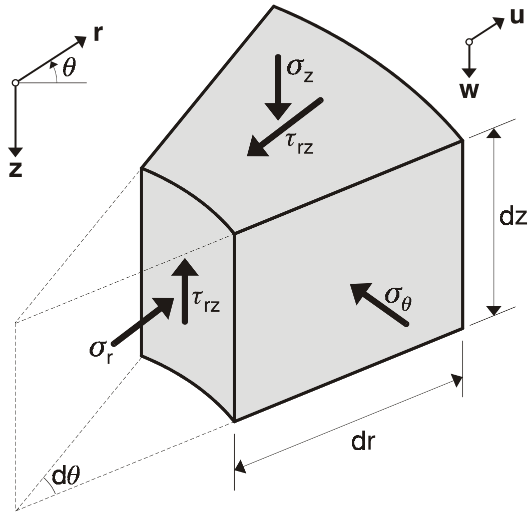

Figure V-40: Stress state in an axially symmetric distribution of stresses (after Vanden Berghe, 2001)

The model considers each soil element as simply sheared (Figure V-41). A shear displacement is imposed between the internal and external shaft of the soil element. Neither axial nor radial normal strain are permitted along these boundaries. The non-vanishing strain of the strain tensor is the shear strain γ_{rz} ($\gamma_{rz} \neq 0$; $\varepsilon_r = \varepsilon_\theta = \varepsilon_z = 0$).

It is assumed that there is no variation of stresses and strains along the z axis ($\partial(..)/\partial z = 0$). The radial normal stress and the shear stress do not change as a function of depth (Vanden Berghe, 2001).

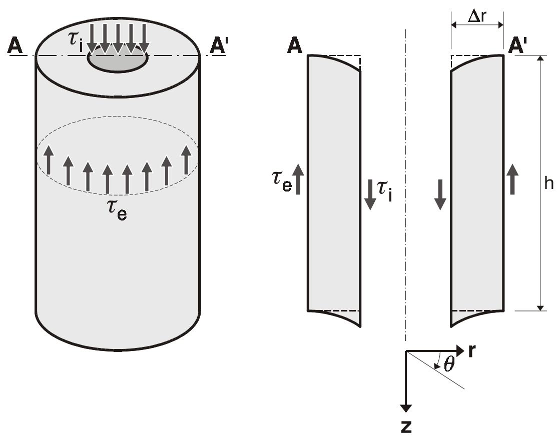

Figure V-41: Simple shearing in axisymetry (after Vanden Berghe, 2001)

Vanden Berghe (2001) showed that the assumptions concerning the stress and strain distributions in cylindrical symmetry are compatible with the equation of equilibrium. The results point out that the assumption of a constant shear strain rate between the middle points of each element was limited to thin elements. The evolution of the shear strain is naturally proportional to 1/r in an elastic and axisymetric media.

3.3. Validation of the model

3.3.1 Propagation of the wave in an elastic media

It would be interesting to check the propagation of a wave in an elastic media by confirming the wave propagation velocity, and the attenuation of the signal during its travel through the elements. The model does not take loading rate effects into account for this reference case, in order to ensure a purely elastic behaviour of the soil reaction.

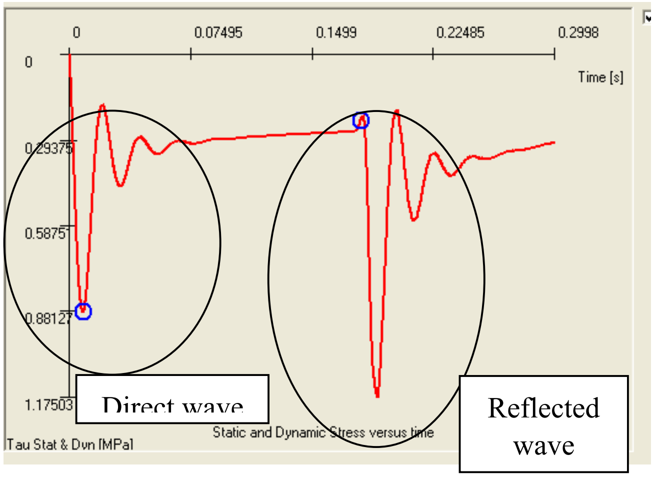

<u>Figure V-42</u>: direct and reflected wave

Since the model is spatially limited and the stress wave is reflected at the outer boundary, this reflection is used to evaluate the wave propagation velocity. In <u>Figure V-42</u>, both little circles point the same position on the wave trace but respectively on the original wave and on the reflected one after one reflection. Since the position of the element is known, the time of travel can be evaluated and compared with the theoretical one (223 m/s). A 3-D image (<u>Figure V-43</u>, distance from pile shaft – time – soil displacement) represents this propagation:

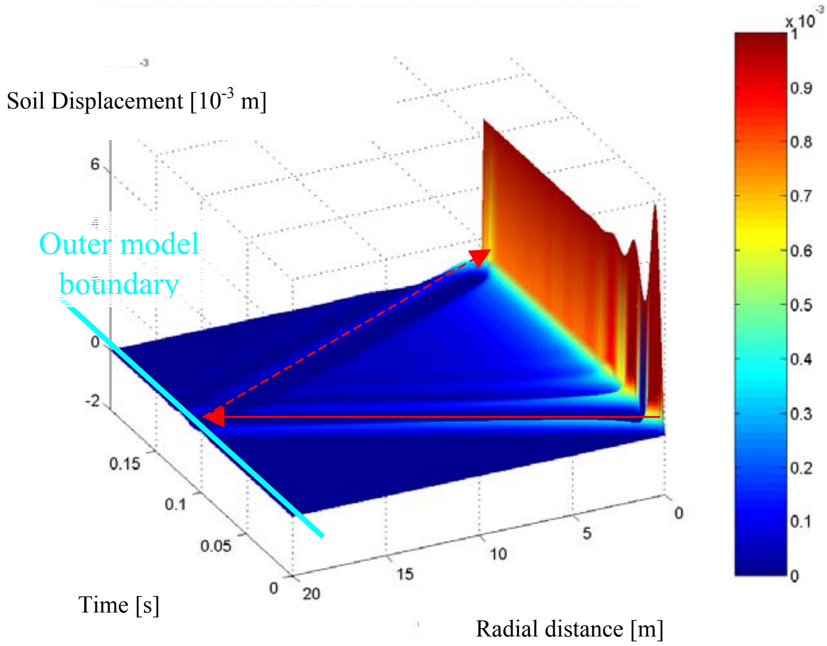

<u>Figure V-43</u>: 3-D representation (time, dist, Displ) of the wave propagation in an elastic soil media with reflecting boundary at r=20m.

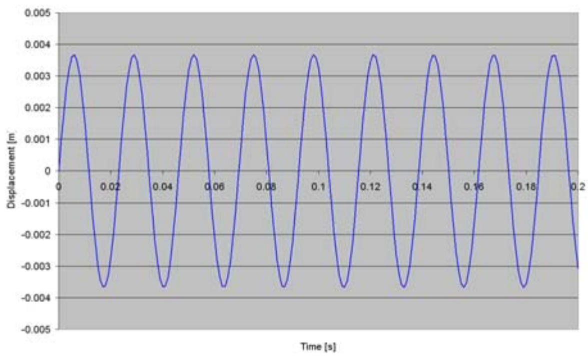

<u>Figure V-44</u>: Periodic displacement of the pile

The second test concerns the attenuation of the signal during its travel. The propagation of a computed wave is compared to the theoretical approach of the soil displacement (Novak et al. 1978 (Equ. II-67)).

To perform this analysis, a harmonic relationship (<u>Figure V-44</u>) is imposed to the pile without predefined attenuation (as the imposed motion introduced in Section 2.3. with the negative exponential function). The stress-strain relationship of the soil is chosen linear and elastic, the ultimate resistance is chosen such as the imposed displacement never reaches it and there is no loading rate effects taken into account.

$v(t)=\cos(\omega t)$ and $u(t)=\dfrac{\sin(\omega t)}{\omega}$ (Figure V-44) **Equ. V-17**

The parameters of the model are:

- Number of elements (cylinders) N_{el}: 400;
- Thickness of each element: 0.1 m → 400x0.1 m = 40 m.;
- Pile radius r_0: 0.2 m;
- Pile length L: 10 m;
- Ultimate static shear resistance $\tau_{ult,stat}$: 1 MPa;
- Poisson ratio υ: 0.35;
- Initial shear modulus G_i: 100 MPa.

And ω = 272 rad/s

The imposed periodic displacement is sent from the pile to the outer border through the soil elements. From element to element, the motion is eased. The attenuation is illustrated by the levels of maximum displacement reached (for each element).

Figure V-45 shows the corresponding generated stress at the interface versus time and versus displacement. It describes the expected displacement-stress relationship.

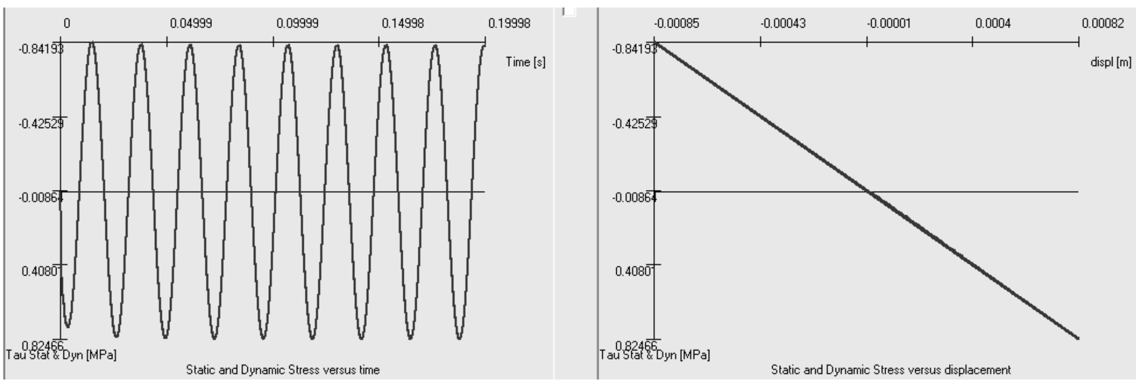

Figure V-45: Time-stress history and displacement-stress history

As expected, the soil element just next to the pile behaves elastically like all the others.

In order to compare the model response to the theoretical Novak approach, the maximum reached points of the traces crossing each element are determined and plotted on a graph vs. the distance between the pile shaft to the centre of the concerned element (Figure V-46).

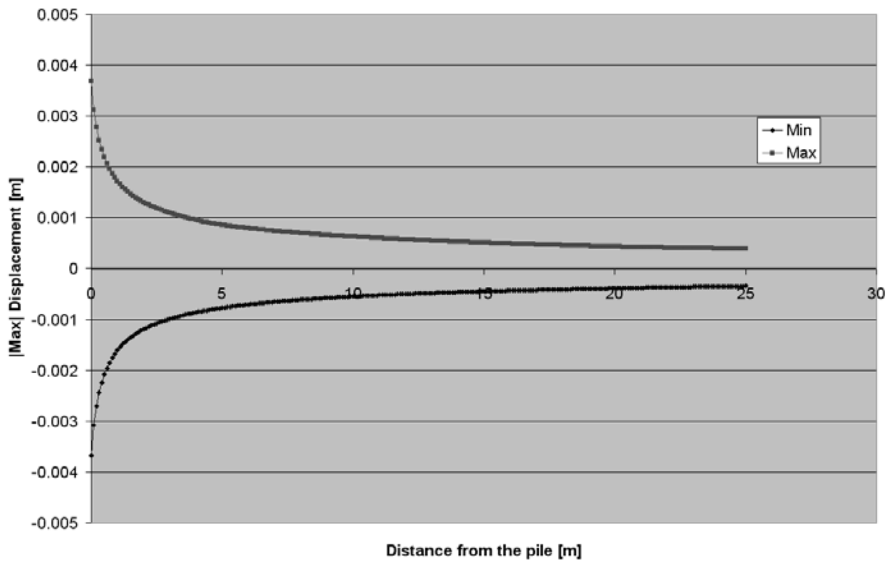

<u>Figure V-46</u>: Maximum and minimum displacements reached for each soil elements under harmonic solicitation around the pile

Equ. II-67 is completed by using the following parameters:

- ω: 272 rad/s;
- r_0: 0.2 m;
- G_i: 100 MPa;
- V_s: 223 m/s.

The development of this equation provides a curve very close to the computed one. <u>Figure V-47</u> shows both curves. The agreement is remarkable and confirms that the model is usable and reliable.

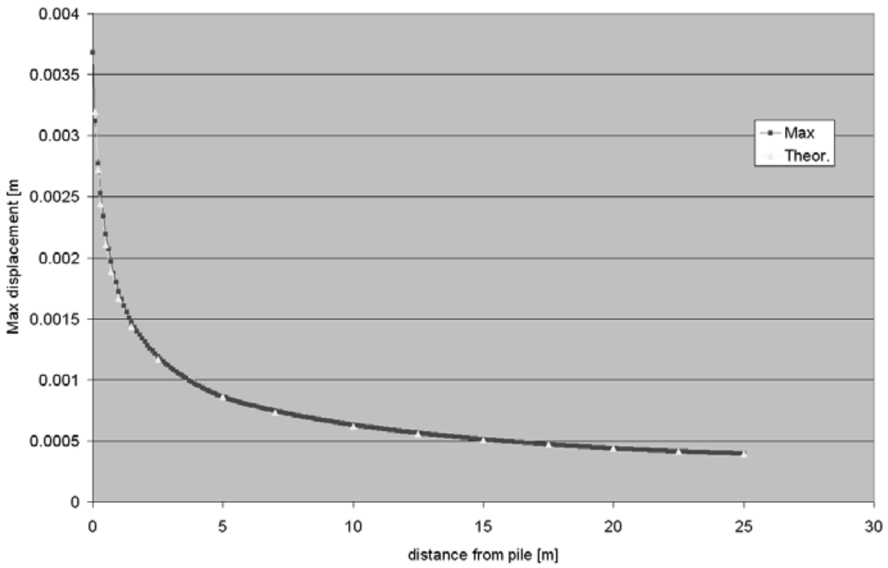

<u>Figure V-47</u>: Curves of attenuations after balancing

Similarly to Figure V-43, a 3D representation of the propagation of a periodic wave is shown in Figure V-48. The tangent of the angle of the yellow "lines" with the time axis represents the wave propagation velocity. The colour "dimension" represents the magnitude of the soil displacement [m].

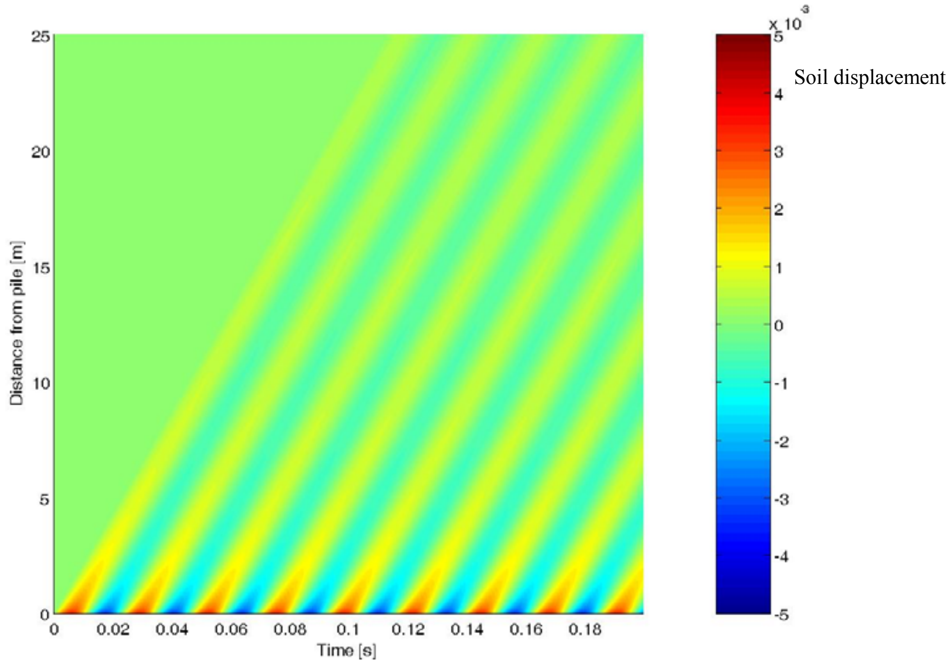

Figure V-48: 3-D representation of the propagation of a periodic wave into the soil (up to 25 m)

3.4. Results

This section presents the results of this model submitted to an imposed motion in order to highlight the slippage event, the slippage zone and the propagation of the wave into the soil.

The elasto-plastic relationship is used to describe the soil behaviour since its performances are well known and the slippage phase is also easier to discern (flat plastic stage).

3.4.1 Elasto-plastic behaviour – no loading rate effects

The parameters used are:

- N_{el} = 300 elements;
- Ring thickness Δr = 0.1 m;
- G_i = 100 MPa;
- Pile radius r_0: 0.2 m;
- Pile length L: 10 m;
- Poisson ratio = 0.35;
- τ_{ult} = 0.3 MPa and 2 MPa

The imposed motion is the harmonic and attenuated signal described in Section 2.3. of this chapter and already used in a previous analysis (Figure V-6).

When the ultimate stress is sufficiently important, the imposed motion can not generate slippage. Figure V-49 to Figure V-52 highlight this situation with the imposed pile displacement, the generated displacement of the first soil element, the generated stress into their interface and the relevant stress-displacement relationship.
As expected, the stress-displacement curve remains altogether linear according to the pure elastic relationship (Figure V-52). Figure V-49 and Figure V-50 plot the imposed pile displacement and the first soil element displacement curves. The trends and the magnitudes of both traces are similar like the permanent settlements. These observations highlight the perfect coupling between the pile and the soil confirmed by the linear stress-displacement relationship. All the information is transmitted from the pile to the soil.

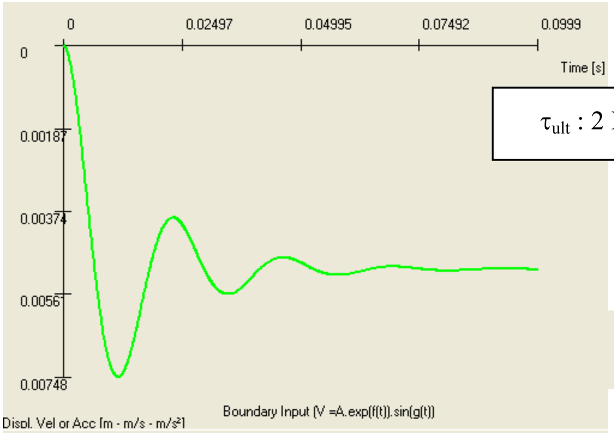

Figure V-49: Input signal imposed to the pile

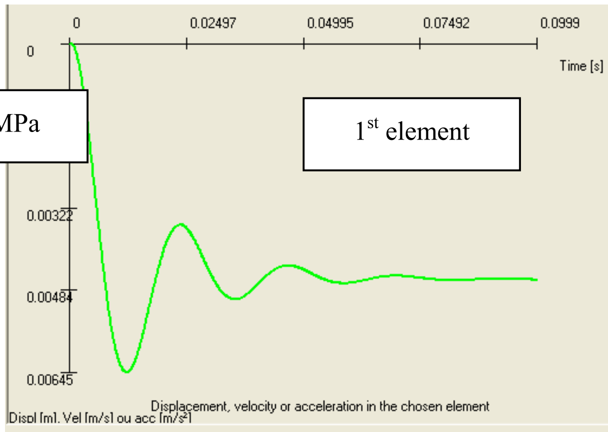

Figure V-50: Generated displacement of the first soil element

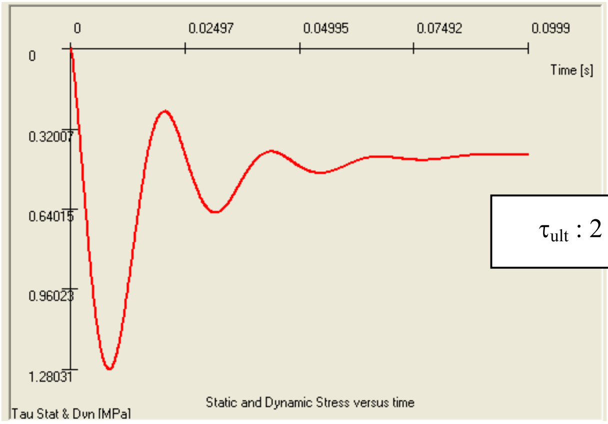

Figure V-51: Generated stress between the pile and the first soil element

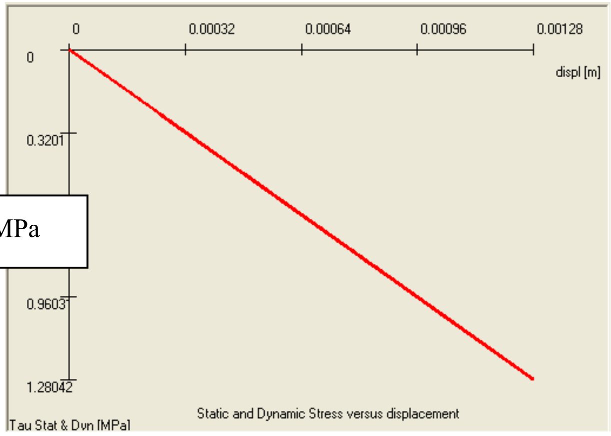

Figure V-52: Displacement-stress relationship (relative displacement)

Figure V-53 displays the displacement traces and the attenuation due to the radiation of the energy into the surrounding soil.

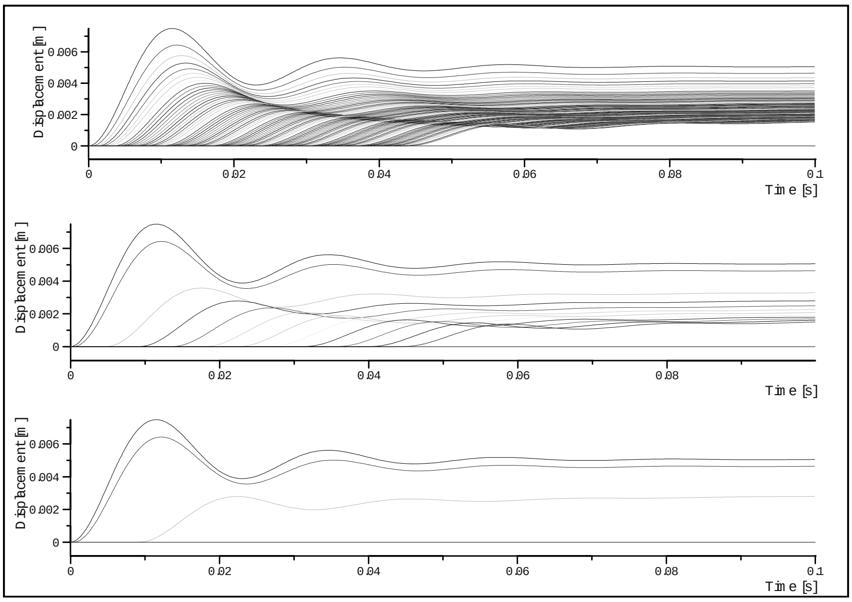

<u>Figure V-53</u>: Displacement traces for the first elements of the model – pile + soil (τ_{ult} = 2 MPa) (a. 100 first, b. 1/10, c. The 1st and the 20th)

The next case takes the slippage into account by reducing the ultimate static stress ($\tau_{ult,stat}$).

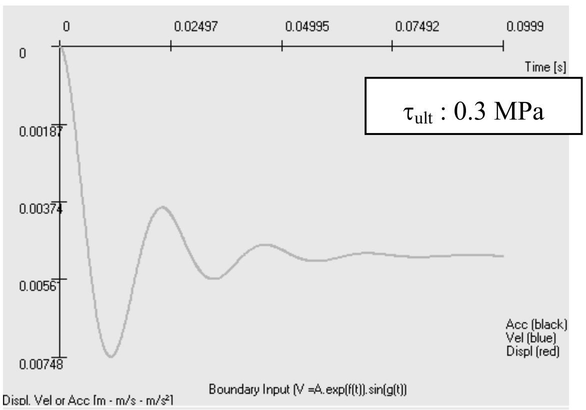

<u>Figure V-54</u>: Input signal imposed to the pile

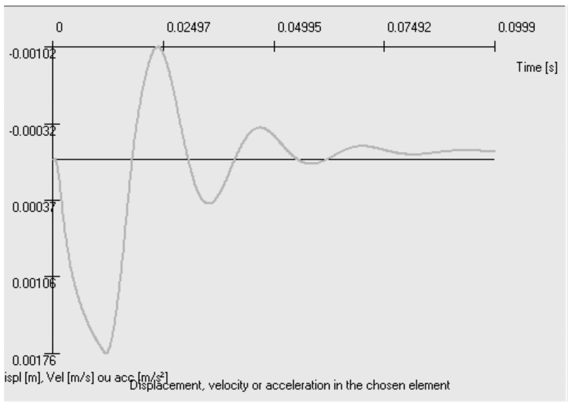

<u>Figure V-55</u>: Generated displacement of the first soil element

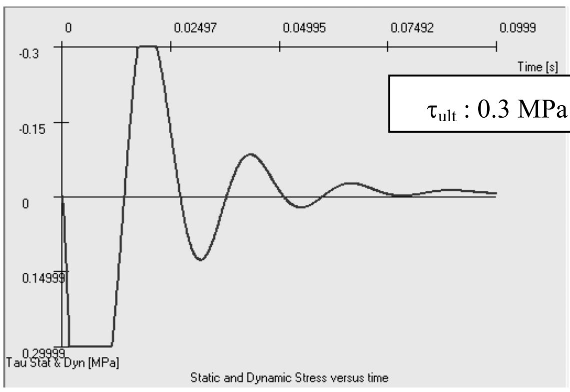

<u>Figure V-56</u>: Generated stress between the pile and the first soil element

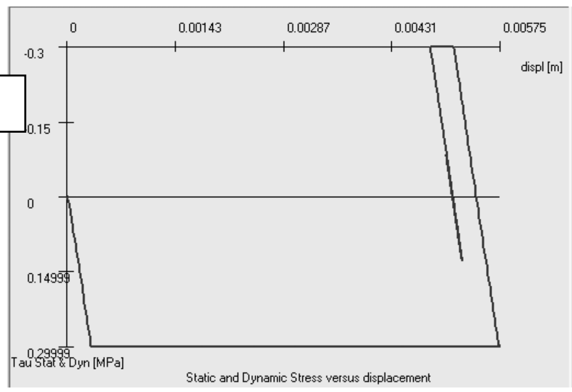

<u>Figure V-57</u>: Displacement-stress relationship (relative displacement)

Similarly to the Figure V-49 to Figure V-52, Figure V-54 to Figure V-57 represent the traces characterizing the pile and the first soil element of the model. The relative displacement between both elements results in a stress resisting to their movements. Due to the small value of $\tau_{ult,stat}$, the ultimate resistance is quickly exceeded and the slippage occurs (Figure V-56).

During the slippage, there is still an interaction between the pile and the first soil element limited to the ultimate shear resistance. This interaction is limited but both pile and soil are not completely uncoupled. Consequently, the motion of the soil element is not interrupted and is based on the stress balance with respect to the equations of motion. This behaviour occurs until the stress between the pile and the soil element becomes inferior to the resistance threshold. Figure V-57 shows the development of the stress vs. the relative displacement of this interface. Nevertheless, the slippage influences the form of the soil displacement. Figure V-54 and Figure V-55 represent the displacements traces of the pile and the first soil element, respectively. It can be seen that both amplitudes and permanent displacements are greatly influenced by the slippage event. The soil element displacement trace is modified. After, this "new" shaped wave is applied to the subsequent soil elements and the coupling is perfect. The slippage has been occurred only in the first interface, the "modified" signal is considered as a new imposed one.

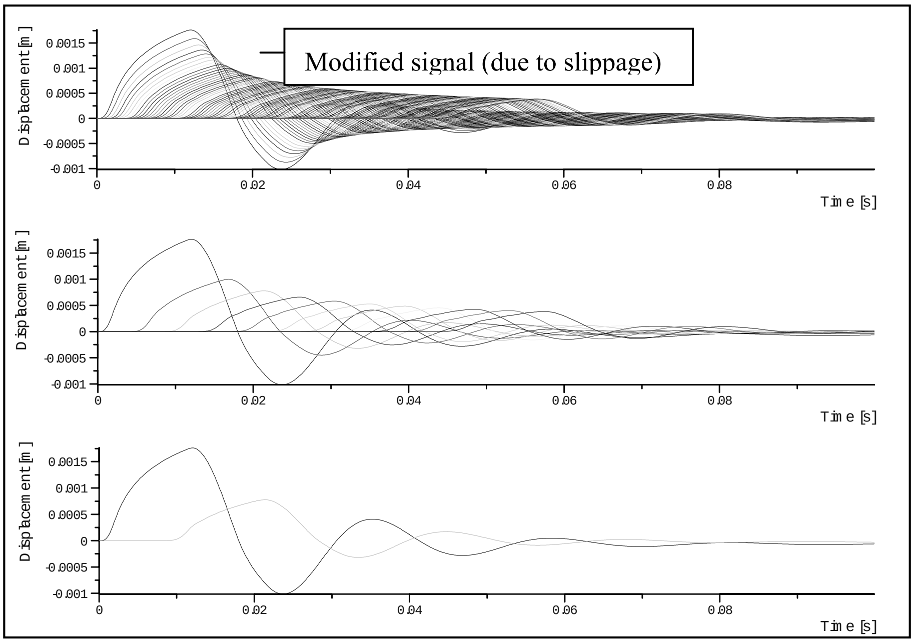

Figure V-58: Displacement traces for the first elements of the model - soil (τ_{ult} = 0.3 MPa) (a. 100 first, b. 1/10, c. The 1st and the 20th)

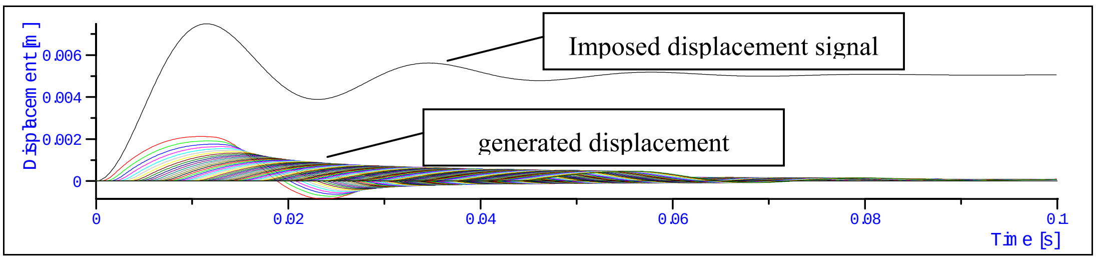

Figure V-59: Displacement traces for the first elements of the model – pile + soil (τ_{ult} = 0.3 MPa) (100 first)

The evolution through the others soil elements is also shown in Figure V-58 and Figure V-59 where all imposed and generated displacements are plotted. The difference and the consequences of the slippage are highlighted by the important gap existing between the pile and the soil displacements.

In conclusion, the slippage occurring between two elements acts like a filter to the propagation of the motion and the resultant stress and not like a barrier.

3.4.2 Elasto-plastic behaviour – Viscous influence

The loading rate influence is located in one stress term called the viscous stress, velocity dependent term and in the ultimate shear stress also a velocity dependent term. The formulations used to quantify these effect are based on the Coyle and Gibson power law (Equ. V-16) with:

- The damping factor of the viscous term (J_s [$s/m^{0.2}$]);
- The damping factor of the ultimate term (J [$s/m^{0.2}$]);

Their values are in this case fixed to $J = J_s = 0.5\ s/m^{0.2}$.

The effects and the probability of slippage are amplified in the first soil elements in the direct vicinity of the pile shaft due to the addition of the viscous contribution to the soil reaction. And the relative velocities are dependent of the slippage state. In case of non-slippage, the difference of velocities between adjacent elements is small. But, on the other hand, during the slippage, the difference becomes higher and influences the threshold of resistance (increase). Figure V-60 shows the amplitude of the absolute velocities of the first elements of the model (pile + soil elements). The maximum magnitude decreases due to the geometric attenuation from the value of approximately 1 m/s (pile velocity) to 0.25 m/s (100th element – 10 m).

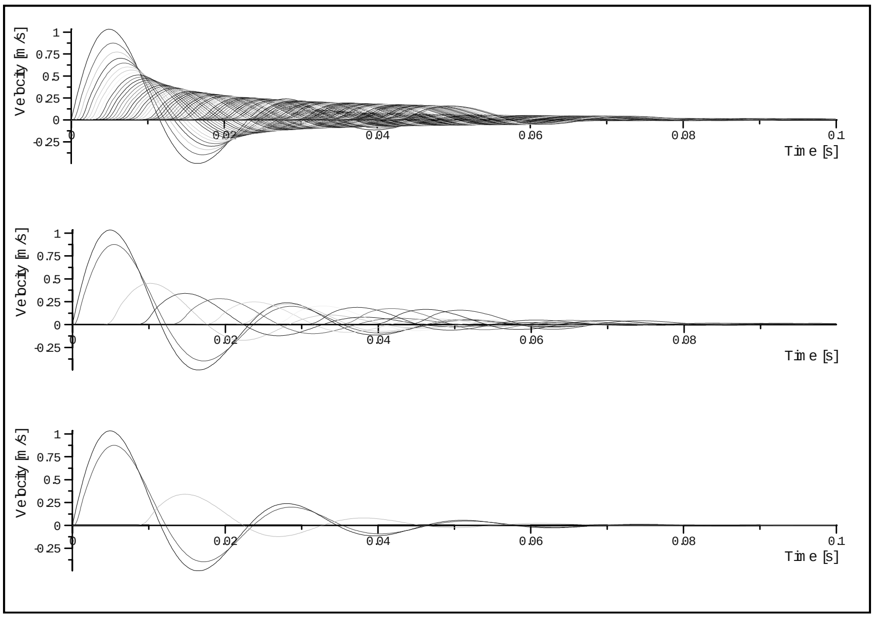

Figure V-60: Velocity traces for the first elements of the model – pile + soil ($\tau_{ult,stat}$ = 2 MPa) (a. 100 first, b. 1/10, c. The 1st and the 20th)

[Figure V-61](#) shows the same simulation results, but expressed in the relative form or the interface velocity (v_{i-1}-v_i). The effects on the rheologic ultimate soil resistance and on the viscous term is an increase of about 10 % of the ultimate static resistance for the elements close to the pile and at 10 m, the increase is only 3% of the ultimate static resistance[1].

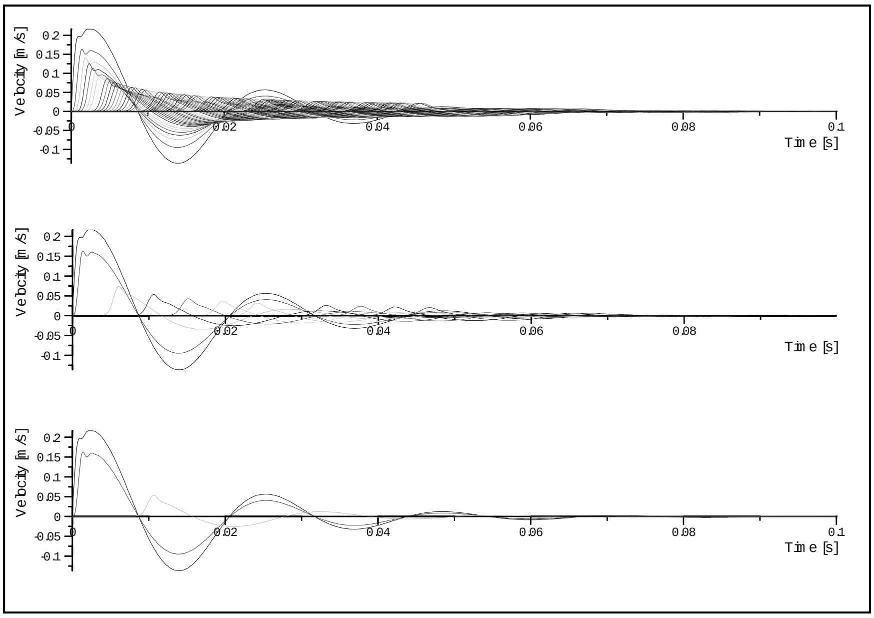

Figure V-61: Relative velocity traces for the first elements of the model ($\tau_{ult,stat}$ = 2 MPa) (a. 100 first, b. 1/10, c. The 1st and the 20th)

Moreover, Figure V-60 and Figure V-61 correspond to a situation of no slippage ($\tau_{ult,stat}$ = 2 MPa). The reduction of the velocity between soil elements follows the geometric attenuation due to the radiation around the pile. If the slippage is provoked by fixing the ultimate shear stress to a small value: 0.3MPa, the influences on the relative velocities are significant. Figure V-62 and Figure V-63 display the velocity curves in the same model configuration than the previous figures and it can be pointed out that the net velocities drop directly through the first interface. Consequently, the relative velocities are also influenced. The first interface velocity is quite large and the following rather small.

[1] With J = J_s = 0.5 s/$m^{0.2}$

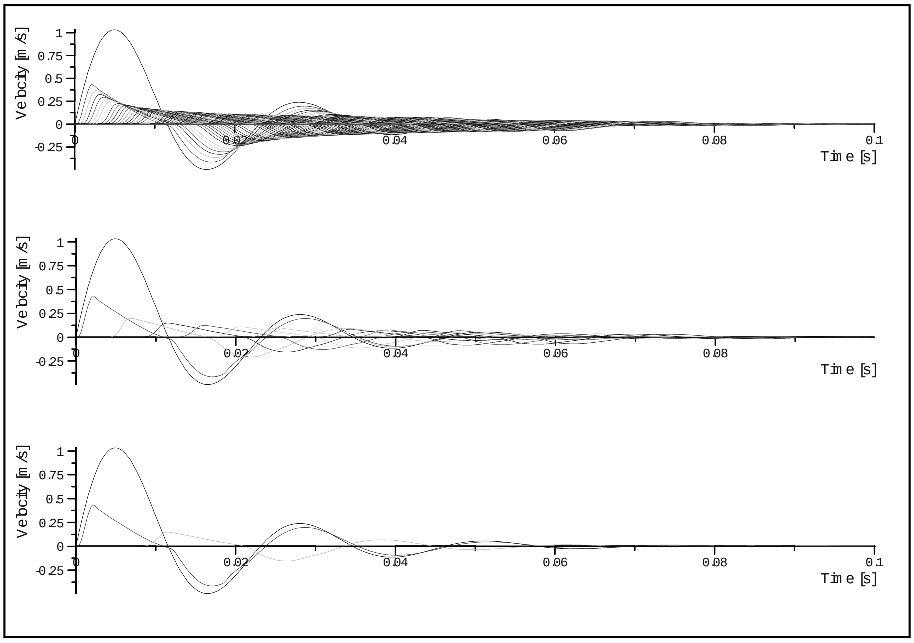

<u>Figure V-62</u>: Velocity traces for the first elements of the model – pile + soil (τ_{ult} = 0.3 MPa) (a. 100 first, b. 1/10, c. The 1st and the 20th)

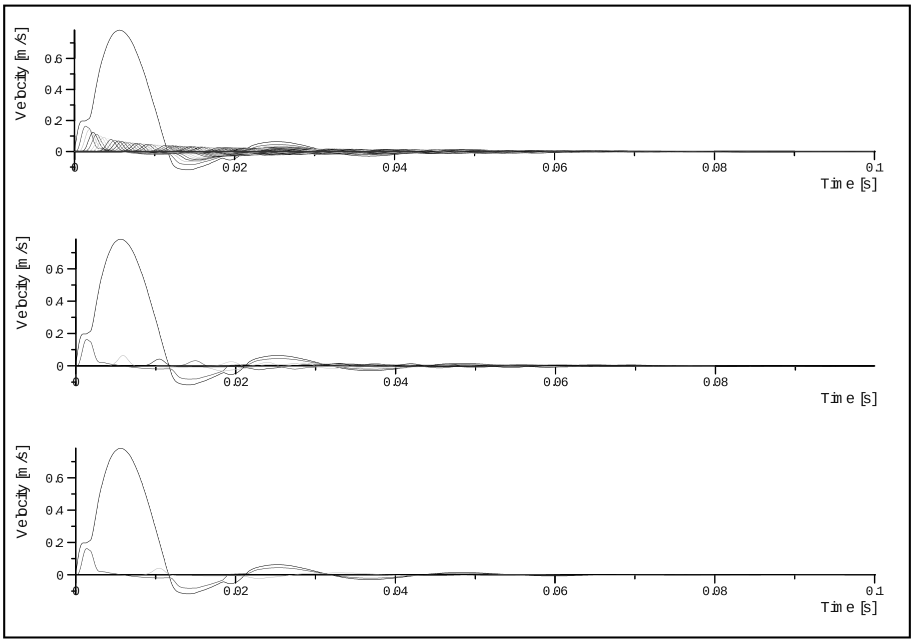

<u>Figure V-63</u>: Relative traces for the first elements of the model (τ_{ult} = 0.3 MPa) (a. 100 first, b. 1/10, c. The 1st and the 20th)

In others words, when the slippage occurs between two elements, the interface velocity increases as the rheologic ultimate soil reaction and the viscous term.

3.5. Depth of the slippage zone

In order to discern if a certain depth of soil or only the interface between the pile and the soil is disturbed by the slippage, a sequence of simulations has been performed in the Cyl model set up to have a sufficient precision in the quantities calculated (small thickness of soil elements) and to avoid reflections at the outer border of the model (N_{el} sufficiently high).

The ultimate static shear stress is fixed in order to ensure the slip ($\tau_{ult,stat} = 0.2$ MPa).

The others parameters are given by:

- $G_i = 100$ MPa ;
- Poisson ratio = 0.35 ;
- Pile length = 10 m;
- Pile radius = 0.2 m.

The stress-displacement relationships of the 7 first interfaces are presented in order to check the propagation of the slippage front. Moreover, to have a better chance to distinguish the slippage occurrence, the fundamental relationship remains the elasto-plastic law.

3.5.1 Static aspect

The first simulation concerns the static term without any loading rate effects.

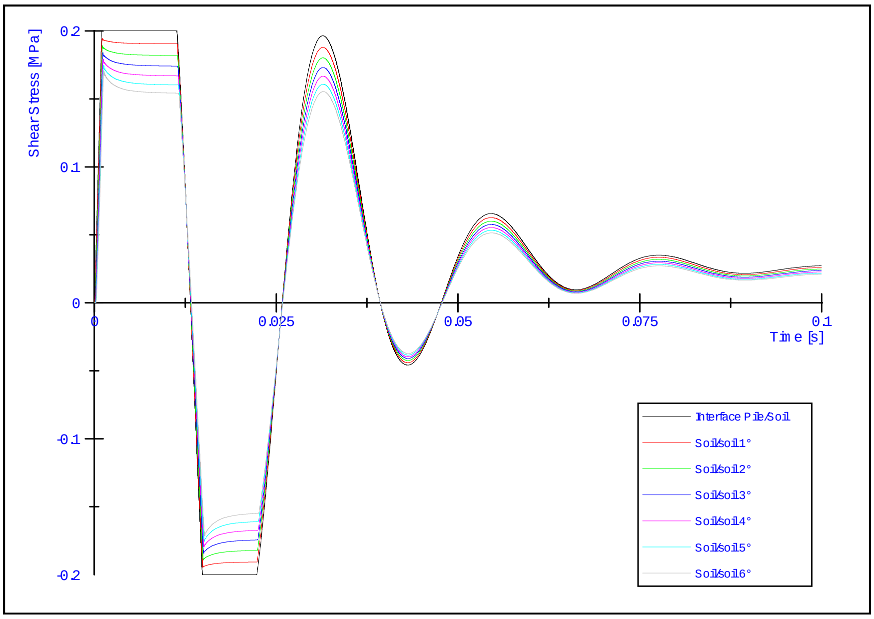

Figure V-64: Static stress behaviour of the 7 first interfaces between pile and soil elements. (τ_{ult} = 0.2 MPa)

Figure V-64 displays that the slippage occurs only at the first interface between the pile and the soil. It was pointed out in section 3.4.1. that the first interface has the role of a moderator or a filter of the transmitted motion. The slippage occurring in this surface reduces the magnitude of the soil motion according to the ultimate soil resistance. The coupled displacement of the soil is maximum equal to the displacement generated by a static stress equal to the ultimate soil resistance. For the following interfaces and soil elements, the attenuation due to the radiation reduces this value with the distance from the pile. Consequently, it is not possible to exceed anew the soil resistance and to generate the slippage in another interface. If the model remains in the static domain, the slippage will remain only at the pile/soil interface. The same event (only one surface of slippage) happens if the ultimate static resistance is reduced by half (0.2 MPa → 0.1 MPa) or doubled.

In conclusion, when only the static part of the soil reaction is taking into account and when the stress follows an elasto-plastic relationship, the ultimate static resistance does not influence the depth of the slip zone but influences the slip duration and the final conditions (pile penetration and residual stresses). Finally, the ultimate stress influences also the shape from stress and displacement traces transmitted to the soil.

3.5.2 Viscous aspect

If a term is added to the static soil reaction which is not related to the stress-displacement relationship, as the viscous term, the slippage front spreading behaviour could be different of the static case.

The viscous influence, velocity dependent, is added to the static soil reaction to generate the rheologic soil reaction limited by the ultimate rheologic resistance of the soil (Equ. V-16). But, as assessed in the model description (Section 3.2) and reminded in Equ. V-16, the same formulation and the same parameter value rules the calculation of both ultimate rheologic resistance and the processing viscous term: J=J_s, the damping parameters. For the convenience, these values are equal even if they represents different behaviours. An analysis could be performed focused on the differentiation of those two values and the consequences on the slippage event.

$$\tau_{rheol,ult} = \tau_{stat,ult} \cdot \left(1 + J \cdot (v_i - v_{i-1})^{0.2}\right) \qquad \textbf{Equ. V-16}$$

$$\& \ \tau_{rheol} = \tau_{stat} \cdot \left(1 + J_s \cdot (v_i - v_{i-1})^{0.2}\right)$$

Since the same formulation and the same parameter rules the ultimate and the viscous contribution of stress, and since this value of J=J_s remains the same for both formulations, both expressions between bracket ("$\left(1 + J_s \cdot (v_i - v_{i-1})^{0.2}\right)$") give the same result for any values of the velocities, the slippage occurs only in case of exceeding the static ultimate resistance. If the static threshold is reached, the ultimate rheologic resistance is exceeded and inversely. A consequence of this observation is the possibility to visualize the effect of the rheologic slippage on the static curves. It is easier and more comfortable to analyse because the rheologic slippage is variable with respect to the time, on the other hand, the elasto-plastic zone of failure is easily identified by the flat portion of the stress-displacement relationship (Figure V-65).

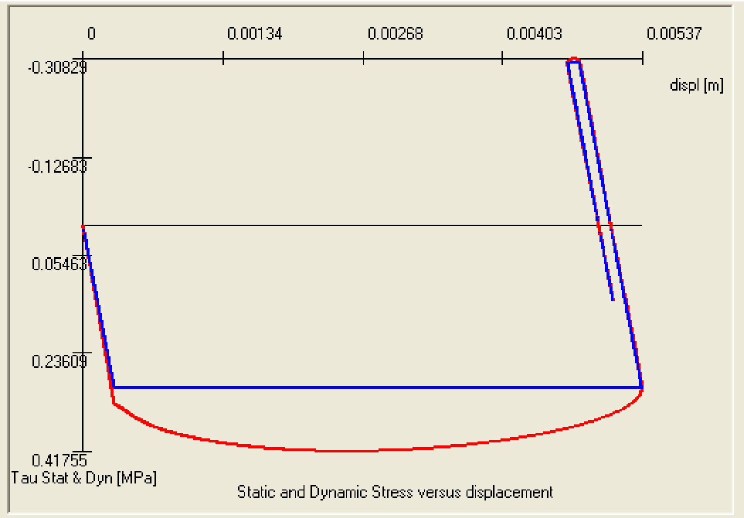

Figure V-65: Generated static (blue) and rheologic (red) stresses-displacement relationships

The rheologic curves are plotted on Figure V-66 (time-static shear stress histories but including to the loading rate effect) and correspond to the pile/soil system of the previous simulation (Figure V-64). The only change is the use of the viscous influence. The sliding occurs, as expected, inside of the first interface but also into the 4 next interfaces between the elements. The slippage is not hold on the first sliding surface along the pile, but can be evaluated in term of number of rings, depth of the slippage zone, parameter values, …The last curve that achieves the slippage is the 4th interface between soil elements. The sliding acts on 5 interfaces (4 between soil elements and one between the pile and the soil), namely on 4 cm.

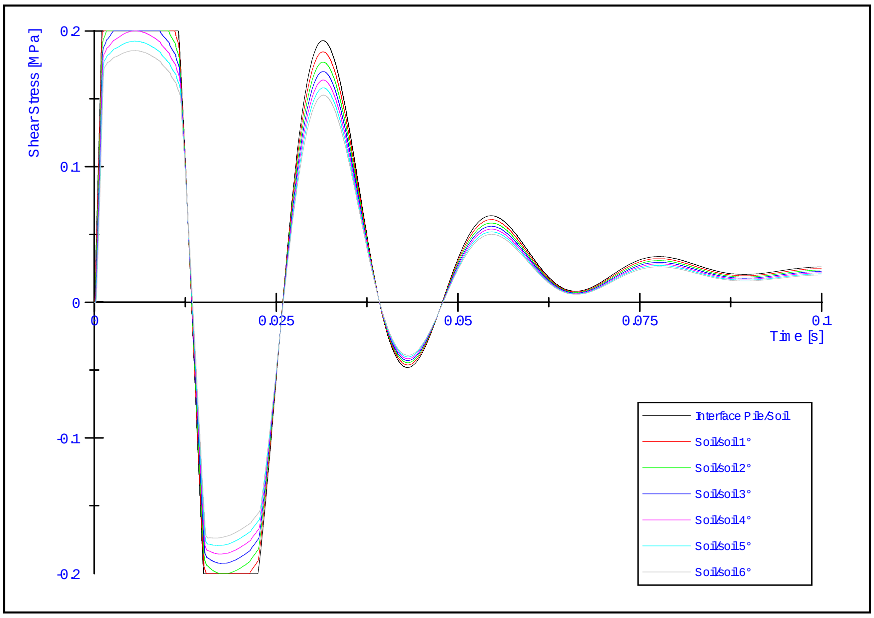

Figure V-66: Static shear stress behaviour of the 7 first interfaces between pile and soil elements - (τ_{ult} = 0.2 MPa, J = 0.5 s/m, e = 0.01 m) – viscous field

If the ultimate resistance is reduced, the sliding depth increases but not in the same proportion than the reduction of resistance. Figure V-67 displays the evolution of the sliding depth for a variation of the ultimate static shear stress (from 0.01 MPa to 2 MPa.). This figure gathers the envelope curves of the maximum reached shear stresses vs. the distance from the pile shaft. A dashed straight line separates the zone where the threshold is reached and where it is not.

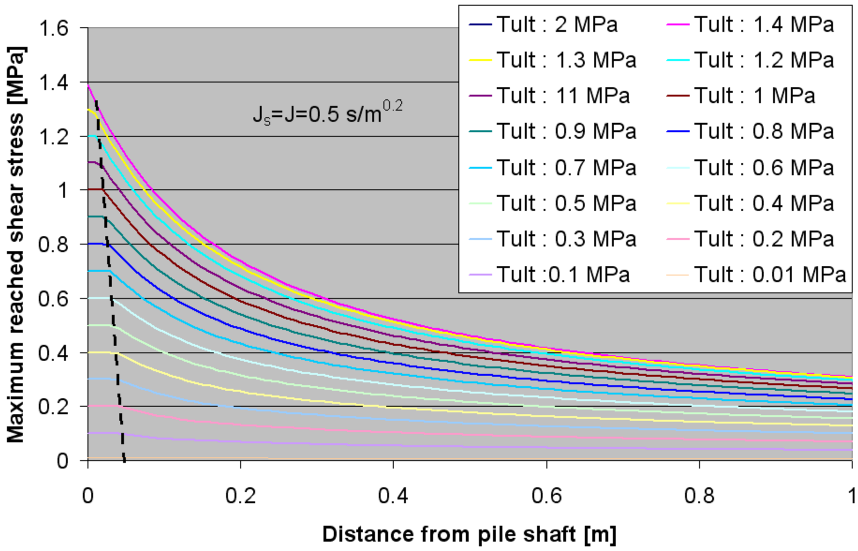

Figure V-67: Curve envelopes of the maximum reached shear stress for τ_{ult} varying from 2 MPa to 0.01 MPa. ($J = J_s = 0.5\ s/m^{0.2}$)

Besides the ultimate resistance $\tau_{ult,stat}$, others parameters have a significant influence on the slippage event. Particularly the value of J (=J_s), the damping parameter: the higher this value, the more spread out the slip zone. Another parameter could influence the slippage area like the damping factor and the ultimate resistance: the initial shear modulus G_i. Since G_i increases the rate of mobilization of the soil, the slip event happens faster and influences the depth of the perturbed zone (increase). The Poisson ratio does not seem to have a significant influence on the depth of the slip zone.

The chosen discretization of the model is still too coarse, and thinner elements could be used to have a more precise description of the perturbed area progression. But the main goal was not to find the exact dimensions of the slip zone, but to evaluate the existence, the progression and the limits of this specific and important failure zone in the vicinity of the pile, by using a simple law (elasto-plastic) without using the particular behaviours probably interacting in this phenomena (increase of pore water pressure, liquefaction, …). Another goal was to find some influential parameters on this perturbation. These parameters are, for the chosen model and the utilized laws, the ultimate resistance τ_{ult} and the damping factor J (for both viscous and ultimate formulations).

It would be very interesting to validate these model observations by a set of laboratory tests on soil samples. Tests like simple shear tests could be easily performed in order to check the real depth and/or the real existence of this zone in the vicinity of the concrete (or steel) contact with the soil. Different shear rates and transducers placed at different distance from the contact into the soil could highlight this important mechanism.

3.6. Detail of the slippage process: about the spreading of the slip zone

This section is dedicated to a detailed explanation of the spreading or not of the slip zone when only the static aspect is taken into account or enhanced with the loading rate influence.

This analysis presents the details of the main quantities involved in the pile/soil and soil/soil responses evaluation. Both cases are detailed separately (specific static point of view and rheologic analysis). the pile/soil system is characterized by the following parameters:

- N_{el} = 2000 elements;
- Ring thickness = 0.01 m;
- G_i = 100 MPa;
- Poisson ratio = 0.35;
- τ_{ult} = 0.2 MPa.
- Pile length = 10 m;
- Pile radius = 0.2 m.

3.6.1 Static field

If the loading rate effects are not taken into account, only the algorithm in Figure V-68-a is followed.

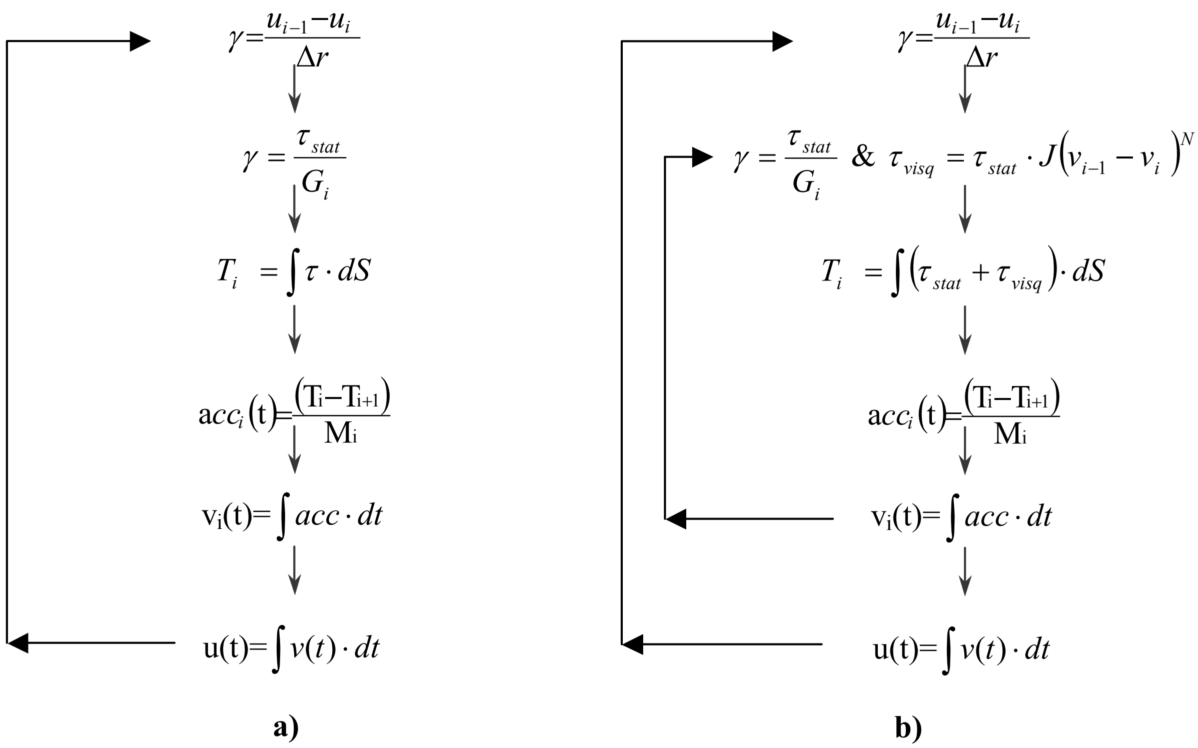

Figure V-68 : Explicit algorithm (static and rheologic aspects)

The used stress strain relationship is the elasto-plastic law:

$$\text{if } \tau_{stat} < \tau_{stat,ult} \rightarrow \gamma = \frac{\tau_{stat}}{G_i}$$

$$\text{if } \tau_{stat} > \tau_{stat,ult} \rightarrow \tau_{stat} = \tau_{stat,ult}$$

The displacement curve (Figure V-69) of the first soil element is highly influenced by the slippage and all the next elements follow this new curve only influenced by the geometric attenuation.

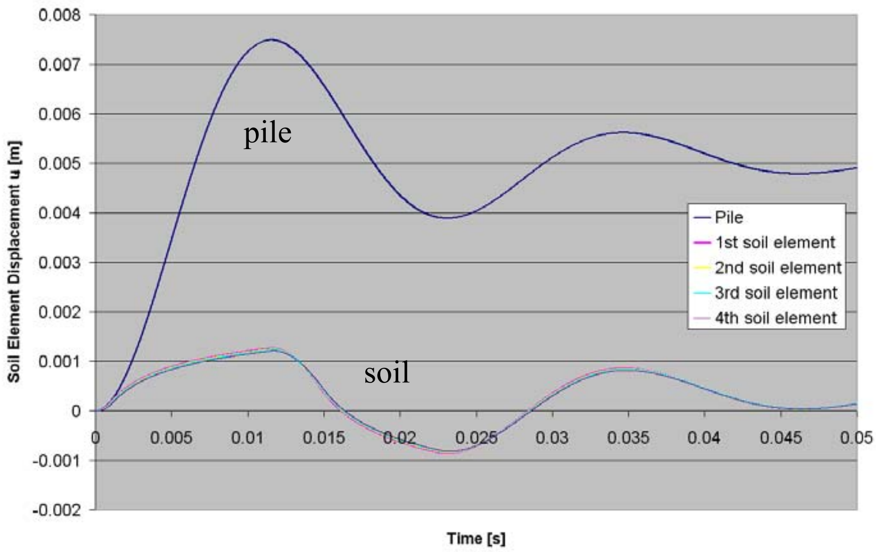

Figure V-69 : Displacement traces of the pile and of the 4 first soil elements - static aspect

If the static threshold is reached, the shear stress into the first interface remains constant (Figure V-70 and Figure V-71). Consequently, it is the same for the corresponding force $T_1 = \int \tau \cdot dS$ Figure V-72 and Figure V-73 for the 1st interface.

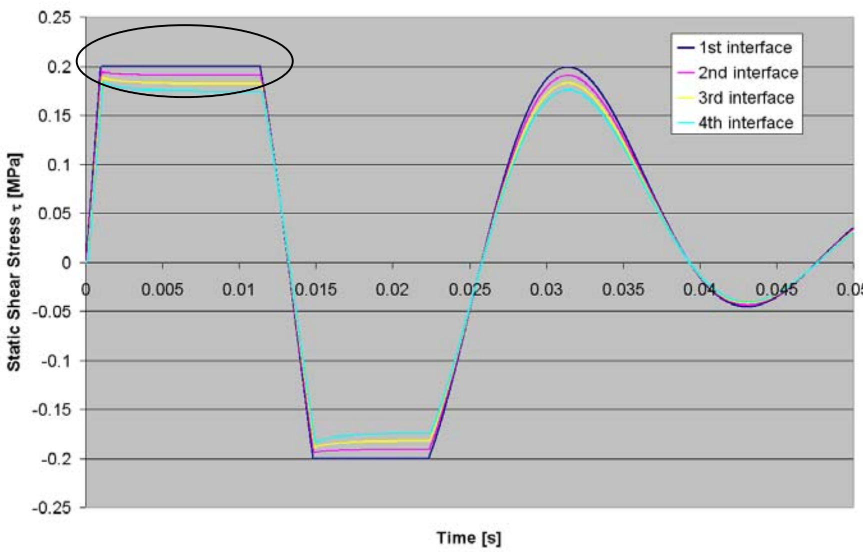

Figure V-70 : Static shear stress traces of the 4 first interfaces - Static aspect

However, during the slippage, the static shear stress curves seem to reach a peak value directly followed by a damped behaviour to an asymptotic value (Figure V-70 & Figure V-71).

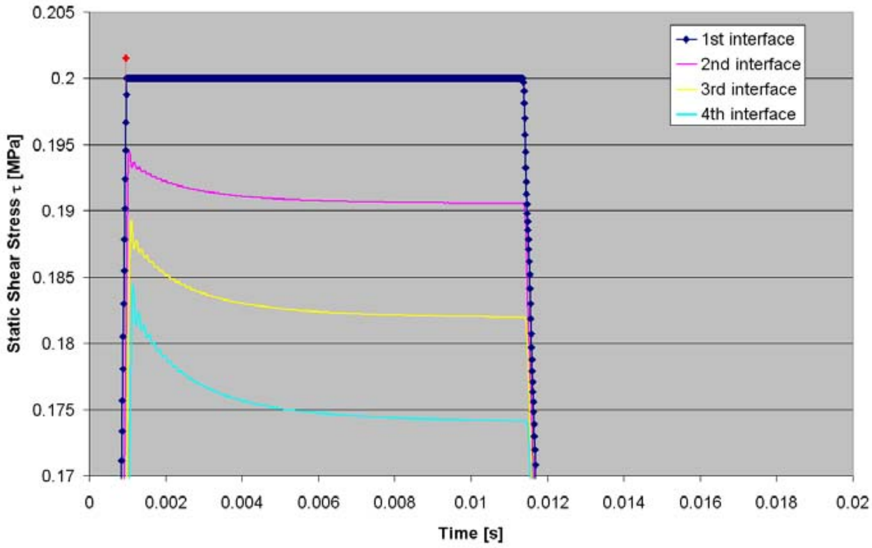

Figure V-71 : Static shear stress traces of the 4 first interfaces - Static aspect – Zoom

In the cylindrical model, all the interfaces forces must be equal (Figure V-72). Since the surfaces of each rings on which the stresses are integrated increases with the distance from the pile, the corresponding stresses must decrease. In these conditions, the ultimate stress can not be exceeded in the farther interfaces and the slippage can not be initiated. This is the main reason of the only slippage in the first interface in a static situation.

When the first interface reaches the ultimate resistance threshold, the natural evolution of the stress should be the red point on Figure V-71. That means that the explicit algorithm stage of the static stress calculation would give this point if the ultimate resistance test of exceeding has not been achieved. Since the numerical test was successful, the stress was limited to the threshold and the blue limit. However, the others interfaces do not reach the ultimate limit at this same time, because they are not in the same position in their own evolution (the transmission of information respects the shear wave propagation velocity in the soil) and because of the geometric attenuation that reduces the corresponding stress with distance. They follow they own behaviour, lead by the imposed pile motion transmitted through the prior soil element until the effect of the first interface slippage event arrives. Since the first interface force is fixed to the ultimate value (T_1 constant) and since the next interface forces are higher, the resulting acceleration becomes of sign opposite to the prior one ($\mathbf{a}cc_1(\mathbf{t}) = \frac{(\mathbf{T}_1 - \mathbf{T}_2)}{\mathbf{M}_1}$), and tends to zero in an oscillating equilibrium. The non sliding interface forces tend to reach the natural position expected with the geometrical attenuation (stress value such the interfaces forces are constant on the model, Figure V-72 and Figure V-73).

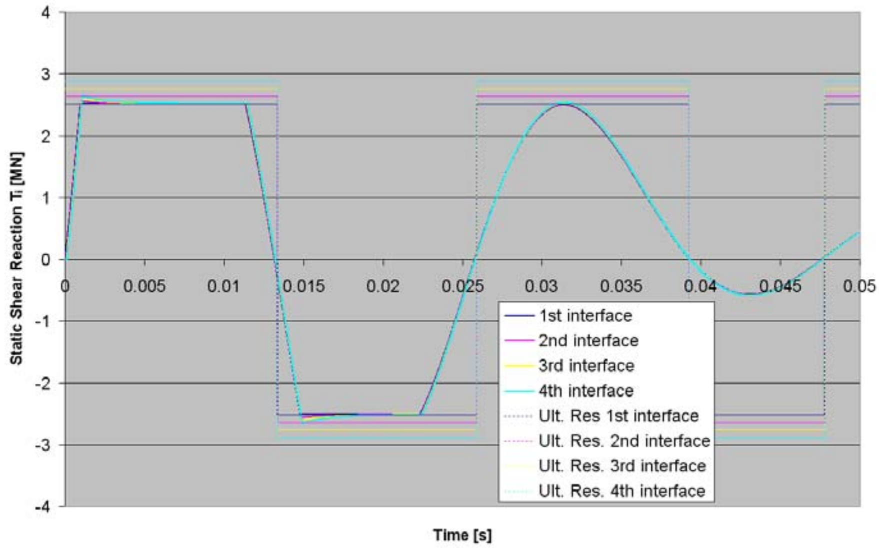

<u>Figure V-72</u> : Static shear soil reaction of the 4 first interfaces (+ corresponding ultimate resistance) - Static aspect

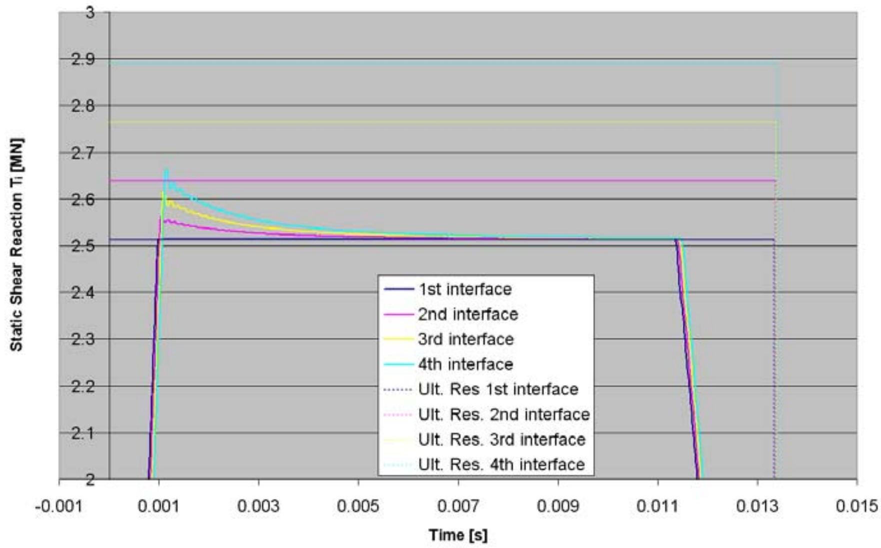

<u>Figure V-73</u> : Static shear soil reaction of the 4 first interfaces (+ corresponding ultimate resistance) - Static aspect - Zoom

<u>Figure V-73</u> highlights that the forces tend to the same value which is the static ultimate resistance of the soil into the first interface. The oscillations disturbing the stress and force displays find their origin in the mechanical behaviour of the spring supposed to model the static behaviour of the soil. The spring associated to the mass of the soil cylinder acts like the static response of the soil but also like a damped Single Degree of Freedom System submitted to an imposed motion. The spring has its own frequency, also called damped frequency, function of its stiffness, of the mass of the element and of the critical damping of the system.

Figure V-74 and Figure V-75 show the velocity results: the soil element velocities and the interfaces velocities. The velocity of the 1st soil element is directly reduced due to the slippage into the 1st interface and the next soil elements velocity traces remain quasi identical to this one.

The interface velocity shows only a significant value for the first interface, during the two periods of slippage. According to Paquet (1988), it could be called the penetration velocity.

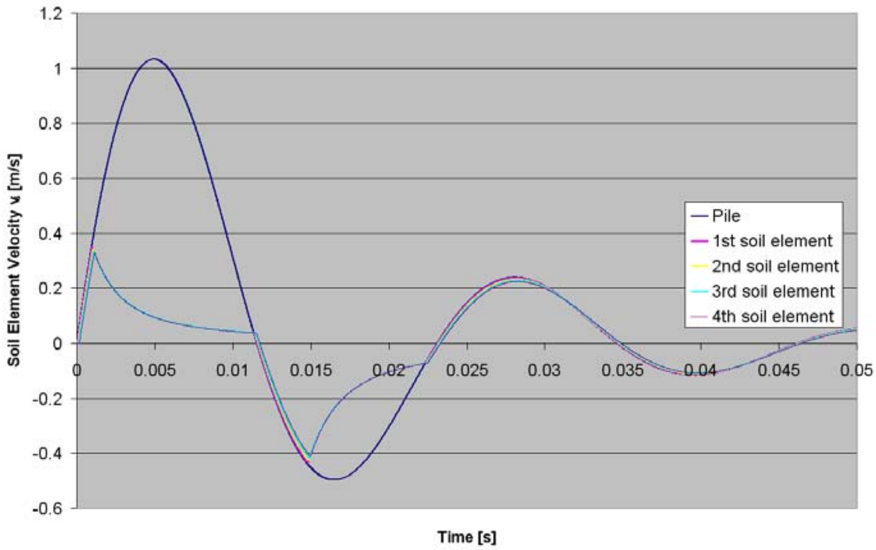

Figure V-74 : Velocity traces of the pile and of the 4 first soil elements - Static aspect

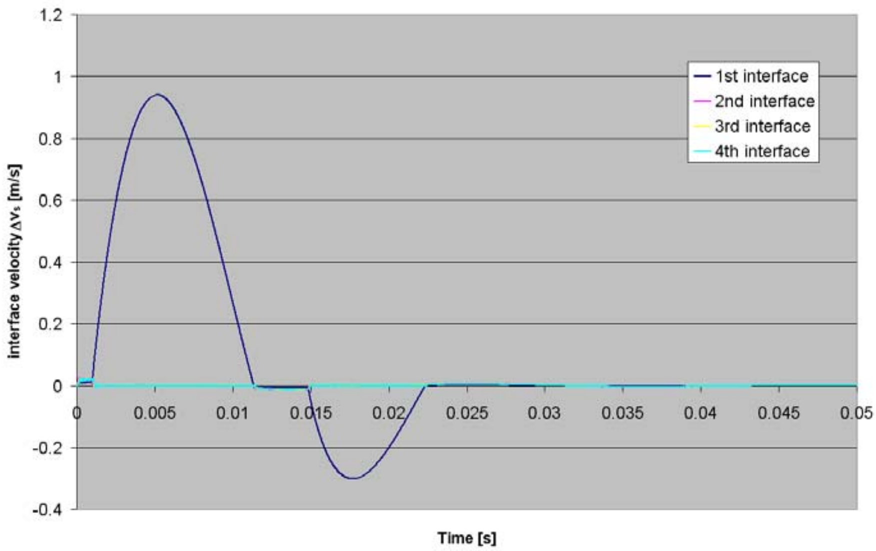

Figure V-75: Interface velocity traces of the 4 first interfaces - Static aspect

3.6.2 Rheologic field

When the use of the viscous contribution to the soil reaction is included, the model response is totally different because a viscous contribution is added to the static term calculated at each time increment.

In the algorithm presented in Figure V-68-b, the eventual exceeding of the ultimate threshold is checked twice per time step: a first time after the calculation of the static shear stress (at each interface) and the second time after addition of the viscous term to generate the rheologic shear stress. After, this stress is integrated and the equations of motion are solved. But, in fine, only the rheologic interface forces are used for the forces balance and the evaluation of the acceleration.

Since the interface forces T_i are larger than for the only static aspect (due to the viscous contribution), the acceleration history is likewise different and so the velocity and displacement histories. Consequently, the static stresses are also influenced. The evolution of the stresses into each interfaces can possibly result in a slippage event not only at the pile/soil interface but also into the next ones depending of the relative weight of the velocity dependent terms. The T_i remain constant along the model, but these forces correspond to the rheologic forces and not the only static ones and includes the displacement and velocity dependent components.

The displacement curves display a progression between the pile displacement and the "static" corresponding curves. Indeed, the curve of the 4th soil element displacement of Figure V-76 presents a similar trend compared to the displacement curves observed for the soil elements in Figure V-69. It is as if the static behaviour was the final state reached after slippage.

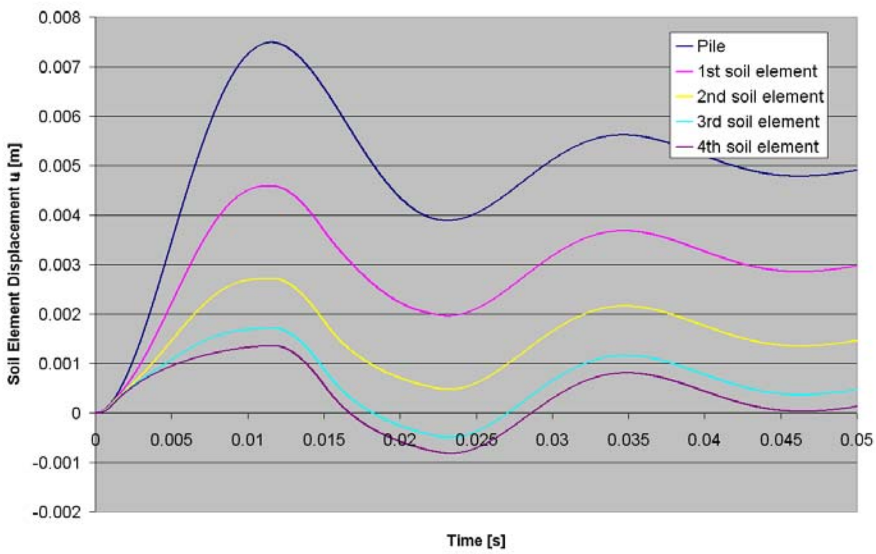

Figure V-76 : Displacement traces of the pile and the 4 first soil elements - Rheologic aspect

Figure V-77 shows that more than one interface reaches the static limit of soil resistance. The figure exhibits also that the consecutive interfaces reach the slippage state with not a constant velocity. The slippage propagation velocities are respectively el#1 → el#2: 45 m/s, el#2 → el#3: 20 m/s and el#3 → el#4: 10 m/s (pronounced marks on Figure V-78). The decrease of velocity points out that the slippage behaviour tends to vanish with the distance from the pile shaft.

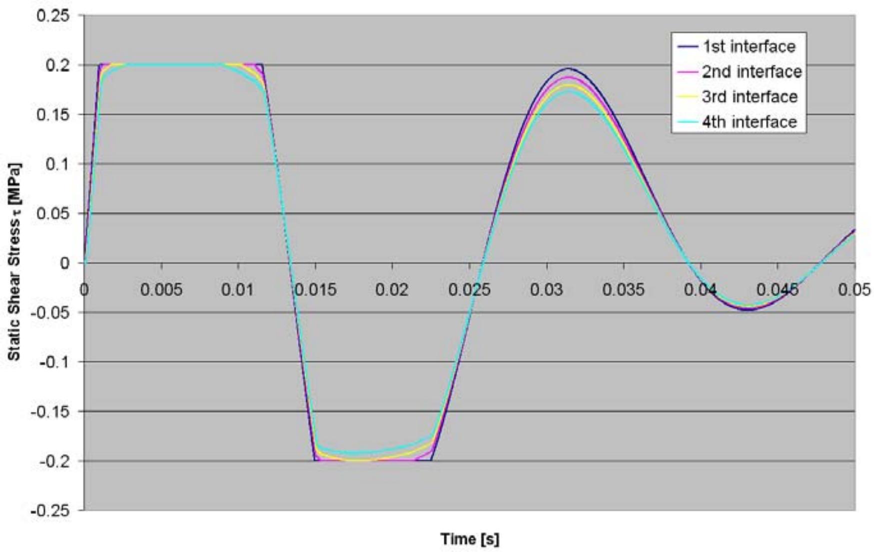

Figure V-77 : Static shear stress traces of the 4 first interfaces - Rheologic aspect

Figure V-78 shows that the static term of the rheologic shear stress reaches four times the ultimate threshold. This is due to the interface displacement which is bigger than in the static aspect due to the addition of the viscous term in the acceleration calculation. All the break points seen on each curves correspond to a direct influence of the prior interfaces when they reached the slip behaviour.

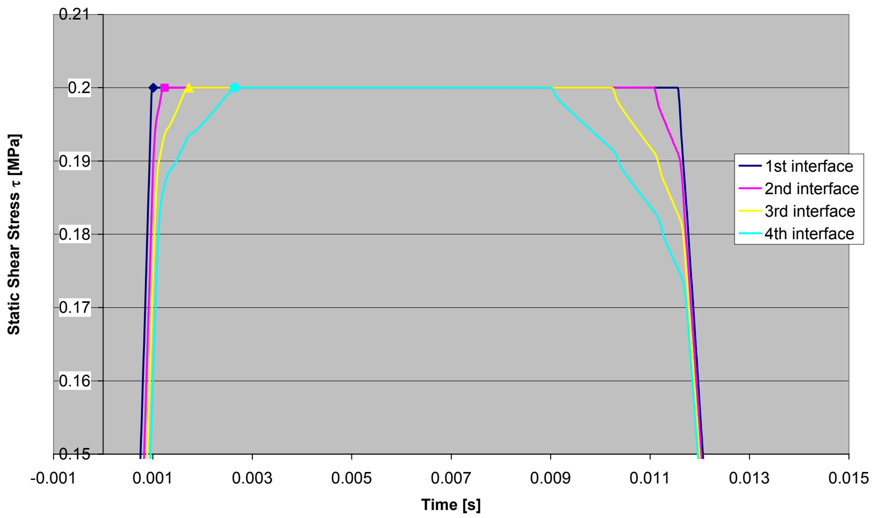

Figure V-78 : Static shear stress traces of the 4 first interfaces - Rheologic aspect – Zoom

Figure V-79 displays the rheologic shear stress influenced by the interface velocity:

$$\tau_{rheol} = \tau_{stat} \cdot \left(1 + J_s \left(v_{i-1} - v_i\right)^{0.2}\right)$$

Since the rheologic parameters J and J_s are identical for the evaluation of the ultimate rheologic shear stress and the rheologic soil reaction, if the static ultimate resistance is reached, it is certain that the rheologic ultimate threshold is also reached

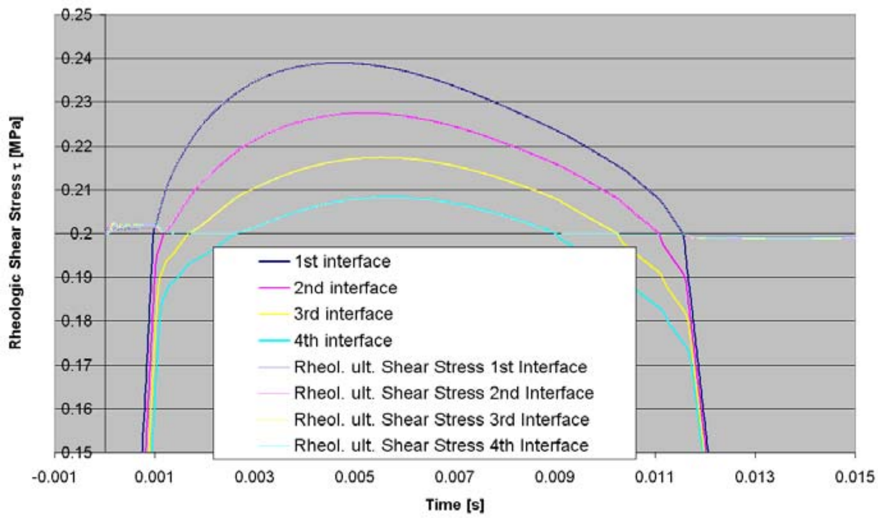

Figure V-79 : Rheologic shear stress traces of the 4 first interfaces (+ Ult. rheol. shear stress) - Rheologic aspect - Zoom

Figure V-80 displays the rheologic interface forces that have to remain constant (after time shifting due to the shear wave propagation).

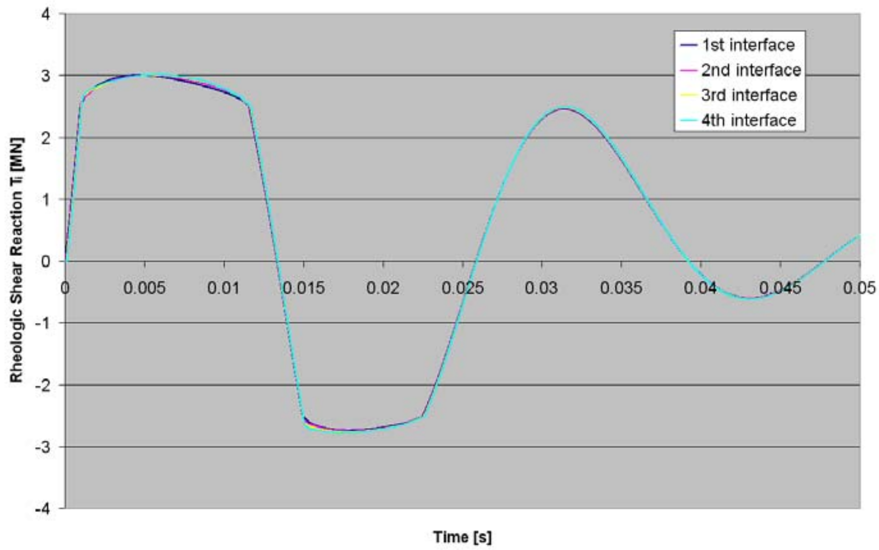

Figure V-80 : Rheologic shear soil reaction traces of the 4 first interfaces - Rheologic aspect

Figure V-81 and Figure V-82 show the velocity results: the soil element velocities and the interface velocities. The soil element velocities acts like the displacement curves. They are in an intermediate situation between the pile velocity and the equivalent velocity of the 1st element in the static analysis. The interface velocities evolves to zero with the slippage condition.

It must be pointed out that the oscillating problems shown in the first part of this section are less present under the rheologic aspect. This is expected because of the use of a dashpot in parallel of the static spring. This mechanical device eases the oscillations.

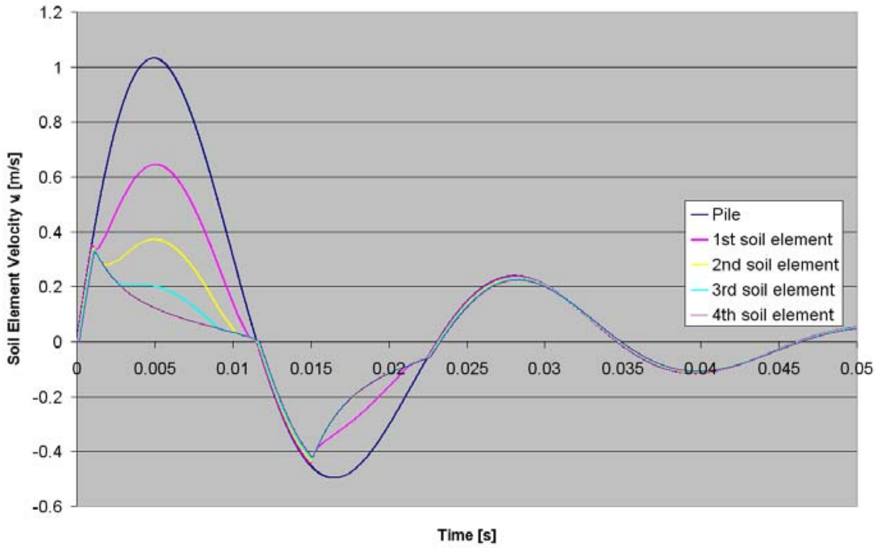

<u>Figure V-81</u> : Velocity traces of the pile and the 4 first soil elements - Rheologic aspect

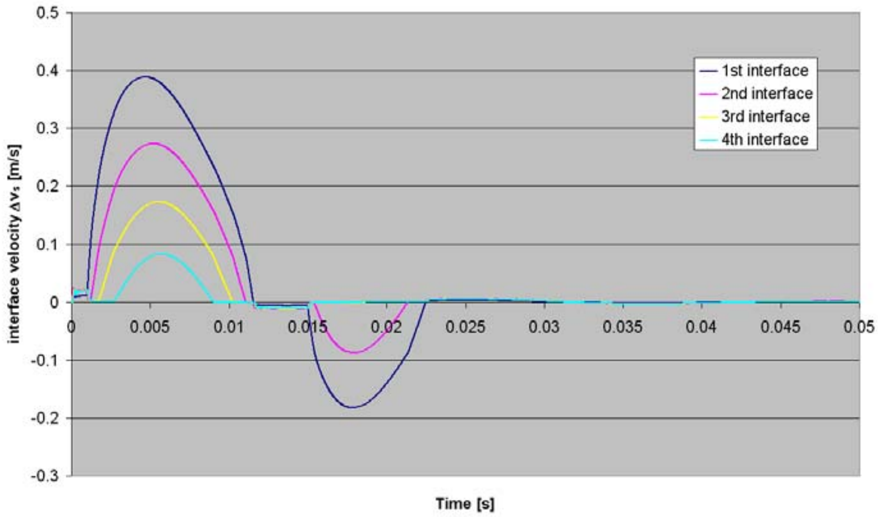

<u>Figure V-82</u> : Interfaces velocity traces of the 4 first interfaces- Rheologic aspect

4. Conclusions

This chapter is dedicated to the slippage event required by the analysis performed on chapter 4. When the soil reaction exceeds a certain limit, the pile must be authorized to slip into the soil. Consequently, both pile and soil motions are differentiated. This requirement needs a modification of the pile/soil model presented in chapter 3 of this thesis. Only the shaft friction modelling is concerned. Two methods were proposed, described and commented to dissociate the pile and the soil motions:

- The DDOF model;
- The Cylindrical model.

The DDOF[2] model only considers the soil reaction in the direct vicinity of the pile shaft. The soil reaction is represented by a static term (≡ a non linear spring and a soil displacement dependent term), a viscous term for the internal dissipation of energy into the soil (≡ a non linear dashpot and a soil velocity dependent term) and a radiation term (≡ a non linear dashpot, function of the mobilization of the static term and of the soil velocity). The ultimate rheologic resistance of the soil beyond of which the slippage occurs, is function of the ultimate static shear stress and of the interface velocity (difference between pile & soil velocities). Since the pile and the soil are perfectly coupled before the soil reaction reaches the limit of resistance, this interface velocity is nil; when slippage occurs, the two media decouple and the resulting interface velocity influences the value of the ultimate rheologic resistance of the soil. During the slippage event, the soil motion is evaluated so that the soil reaction perfectly balances the ultimate rheologic resistance.

This method was developed and implemented in an explicit method. In order to analyse the results, a simplified pile/soil model was created in which a defined motion is imposed to a rigid pile installed in a single soil layer. The curves of soil displacement and velocity were compared to the pile displacement and velocity traces. The corresponding difference is defined as the pile penetration and the penetration velocity. The same approach was found in the model of Paquet (1988) who defined similarly the pile penetration and the penetration velocity.

This model keeps the advantages of the SDOF model (size, simplicity, time computing) and allows to distinguish the pile and soil displacement histories. The pile settlement, governed by the loading, is often longer than the settlement to be followed by the stress-displacement fundamental relationship. Since this information was of importance in the back-analysis and especially in the optimisation of the unloading parameters, the next step required is to validate this approach by implementing the complete pile/soil model (shaft + base) and back-analysing some real dynamic measurements with the algorithm developed in chapter 4. Unfortunately, it was not possible to perform it within this research due to a lack of time.

For a same imposed pile motion, the soil motion, and consequently, the pile penetration are strongly influenced by the choice of the ultimate static resistance and by the value of the damping parameter

[2] Double Degree Of Freedom Model

$J_{(s)}$. This parameter, used in both expressions of the ultimate rheologic resistance (J) and in the viscous term formulation (J_s) with the same value must be differentiated (two different values) what seems to be more logical because both formulations represent different behaviours.

Unfortunately, these observations are only the result of simulations and can not be confirmed by real measurements. There is a need of data allowing to discern the static, viscous and rheologic behaviours along the pile shaft under large strains.

The Cylindrical (Cyl) model describes the soil reaction by mean of concentric cylinders surrounding the pile. The cylinders are a set of rings with the same thickness and an increasing height. The last ring closes the model by an absorbing boundary respecting the theory of Novak et al, 1978. The Cyl model allows the computing of the displacements and the stresses induced in the soil due to a dynamic pile solicitation. The static soil reaction is completed by a viscous term function of the relative velocity between soil elements and the geometry of the model is supposed to represent the radiation term usually modelled in the 1D pile/soil system. This model was developed to highlight the slippage event and its major parameters. The loading rate influence is also marked in the ultimate rheologic resistance of the soil which is also function of the interface velocity.

The model is firstly validated by comparison of results obtained from a simulation with the theoretical approach of Novak et al., 1978. Afterward, the slippage occurring at the interface between pile and soil is described in function of the soil reaction terms authorized to be mobilized.

If only the static terms are used, the slippage is confined to the sole interface between the pile and the soil. On the other hand, if the velocity dependent terms are added to the static soil reaction, it appears that the slippage can spread out in a certain depth around the pile (between soil elements). This depth is function of the ultimate static resistance, of the rheologic parameters (like the ultimate and the viscous damping factors J and J_s) and of the initial shear modulus of the soil. The development of the slippage beyond the pile/soil interface is due to the velocity dependent terms and especially to the viscous term.

Another observation of importance is the fact that despite the slippage, a certain information (a certain motion or energy) goes through the slip surface and propagates into the soil. The slippage is not modelled as an insurmountable barrier but acts as a filter defined by the ultimate soil resistance and stiffness and the rheologic parameters: the smallest the ultimate soil resistance and the faster the mobilization of the soil, the less the transmitted information. A zone of slippage develops around the pile and is determined by the loading rate.

According to its relative weight in the definition of the slippage event and consequently in the development of the shaft friction failure, there is a need to complete the knowledge of the velocity dependent viscous stress. As corollary, a better knowledge of the velocity of which this term is relevant is also required because the choice of the pile, the soil or the interface velocity has a strong influence upon the viscous stress influence on the pile/soil response.